Lead Article

Acta Cryst. (1991). B47, 561-580

Crystal Chemistry of Six-Coordinated Silicon: a Key to Understanding the Earth's Deep Interior*

BY LARRY W. FINGER AND ROBERT M. HAZEN

Carnegie Institution of Washington, Geophysical Laboratory and Center for High Pressure Research, 5251 Broad Branch Road NW, Washington, DC 20015-1305, USA

(*Received* 26 *November* 1990; *accepted* 8 *April* 1991)

Abstract

A survey of high-pressure silicates reveals 12 distinct high-density structural topologies with octahedral Si. Seven of these structure types - stishovite, perovskite, ilmenite, hollandite, calcium ferrite, pyrochlore and K_2NiF_4 type - contain only six-coordinated silicon. Other high-pressure silicates, including those with the garnet, pyroxene, wadeite, anhydrous phase *B* and phase *B* structures, contain both tetrahedral and octahedral Si. Five systematic trends among these dozen structures suggest the existence of other, as yet unobserved, possible mantle Si phases. The criteria are: (1) structures like rutile, hollandite and calcium ferrite formed from edge-sharing chains of silicon octahedra; (2) germanates synthesized at room pressure with octahedral Ge; (3) isomorphs of room-pressure oxides with 3+ or 4+ transition-metal cations; (4) high-pressure magnesium silicates related to room-pressure aluminates by the substitution $2Al \rightarrow Mg + Si$; and (5) the homologous structures in system Mg-Si-O-H that includes phase *B* and anhydrous phase *B*. Each of these criteria can be used to predict other potential octahedral Si phases. Of special interest are predicted structure types that fulfill more than one criterion: diaspore-type $(MgSi)O_2(OH)_2$, aerugite-type $Mg_{10}Si_3O_{16}$, sphene-type $CaSi_2O_5$, benitoite-type $BaSi_4O_9$, gibbsite-type $MgSi(OH)_6$ and pseudobrookite-type Fe_2SiO_5.

Introduction

Silicon and oxygen are the most abundant elements in the earth's outer layers. Silicates comprise the commonest minerals on the earth's surface and presumably they dominate throughout the earth's mantle (to a depth of about 2900 km). Many hundreds of silicate structures have been determined and catalogued (see *e.g.* Liebau, 1985), but only about 50 different structures account for the vast majority of all crustal silicates (Smyth & Bish, 1988). A common feature of all these low-pressure mineral structures is the presence of silicon cations exclusively in four coordination ($^{[IV]}Si$) by oxide anions. The polymerization of SiO_4 groups dictates many mineral properties and it provides the basis for most silicate classification schemes.

Research on silicates synthesized at high pressures and temperatures plays a major role in our efforts to understand the earth's deep interior. Cosmochemical assumptions regarding the earth's bulk composition, coupled with seismological investigations of radial inhomogeneities, establish important constraints for modeling our planet. Even so, actual crystalline materials, erupted from depths of more than 100 km or produced in high-pressure laboratory apparatus, provide our best opportunities for deriving a detailed picture of the inaccessible 99·8% of the earth's solid volume. The first experiments on common rock-forming silicates at pressures up to 10 GPa (100 kbar or approximately 100 000 atmospheres) revealed striking changes in mineral structure and properties. Sergei Stishov's seminal investigation of SiO_2, for example, demonstrated the transition from a relatively open quartz framework of corner-sharing silicate tetrahedra to the dense rutile-type structure of stishovite with edge-sharing chains of silicate octahedra (Stishov & Popova, 1961). The corresponding increase in density - more than 66%, from 2·65 to 4·41 g cm^{-3}, between 0 and 8 GPa (Ross, Shu, Hazen & Gasparik, 1990) - has profound implications for interpretation of seismic velocity data.

Subsequent high-pressure experiments have demonstrated that all common crustal silicates undergo phase transitions to new structures with six-coordinated silicon ($^{[VI]}Si$) at pressures between 8 GPa (for pure SiO_2) and about 30 GPa, which corresponds to the pressure at the top of the earth's lower mantle. Many researchers now assert that the dominant mineral structure type in the earth's lower mantle - indeed, the structure that may account for more than half of the solid earth's volume - is perovskite of the approximate composition $(Mg_{0.88}Fe_{0.12})SiO_3$, in which silicon occurs in a corner-linked array of octahedra. Silicate perovskites,

* *Editorial note*: This invited paper is one of a series of comprehensive Lead Articles which the Editors invite from time to time on subjects considered to be timely for such treatment.

0108-7681/91/050561-22$03.00

mixed with the oxide magnesiowüstite (Mg,Fe)O, are thus believed to account for the relatively high seismic velocities of this region, from 670 to 2900 km, in which velocities increase smoothly with depth (Fig. 1). Mineral physicists identify silicon coordination number as the major crystal-chemical difference between the earth's crust and lower mantle: silicon is virtually all four-coordinated above about 250 km, but is entirely six-coordinated below 670 km.

The upper mantle and transition zone, which lie above the lower mantle, possess a much more complex seismic character with depth. This region, extending to a depth of 670 km, displays several discontinuities and changes in slope of the velocity-depth profile (Fig. 1). Such features might be caused by either compositional variations or phase transitions. However, given the suspected pattern of mantle convection and the well documented variety of high-pressure phase transitions in silicates, the latter explanation seems the more plausible. Specific phase transitions have been proposed for each of the major seismic features and mineralogical models have been proposed that account for most of the complexities between 200 and 670 km (Fig. 2).

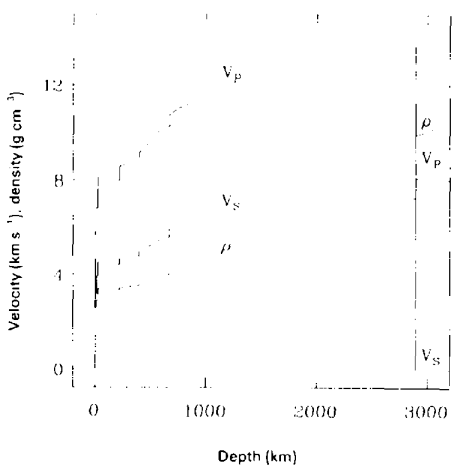

Fig. 1. Velocity-density profile for the earth's crust and mantle.

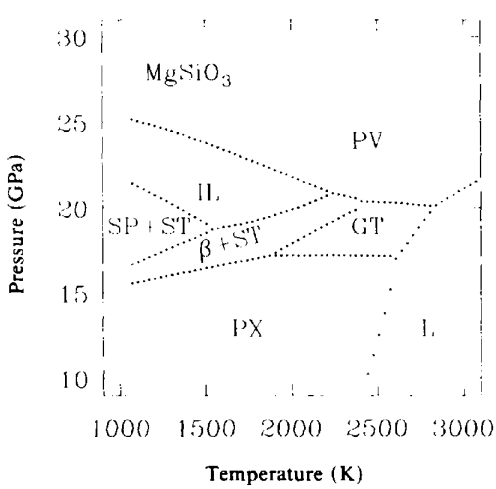

Fig. 2. The phase diagram for $MgSiO_3$ reveals three $^{[VI]}$Si phases - perovskite (PV), garnet (GT), and ilmenite (IL) - as well as pyroxene (PX), spinel (SP), stishovite (ST), β-Mg_2SiO_4 (β) and liquid (L) (from Fei *et al.*, 1990).

One of the most fascinating aspects of the earth's transition zone is the appearance of a group of high-pressure silicates with both $^{[IV]}$Si and $^{[VI]}$Si. The stability of these minerals is apparently confined to a rather narrow pressure range from approximately 10 to 30 GPa. Within these limits, however, are silicate structures of remarkable complexity and great topological interest. Five mixed-coordination high-pressure silicate structures are now known for relatively simple chemical systems that contain Si and one or two other cations, but recent high-pressure experiments on more-complex systems suggest that many other mixed silicon coordination structures may await discovery.

While earth scientists have studied six-coordinated silicon in high-pressure environments, other researchers have focused on an intriguing group of room-pressure synthetic silicates with $^{[VI]}$Si. When coupled with other electronegative cations such as phosphorus or carbon, silicon can become an octahedrally coordinated network former. Polyhedra in these unusual materials tend to be linked entirely by corner sharing (*i.e.* O atoms are two-coordinated), thus leading to framework structures quite distinct in character from the high-pressure silicates of the earth's deep interior, all of which have O atoms in at least three coordination. Octahedral corner sharing also occurs in a variety of organic molecular crystals with $^{[VI]}$Si (see, for example, Flynn & Boer, 1969) and there are several dozen silicon-organic compounds for which $^{[VI]}$Si occurs in aqueous solution (Liebau, 1985). Molecular crystals with six-coordinated silicon are not considered in this review.

The objectives of this review are to describe all known non-molecular silicate structures with six-coordinated or mixed-coordinated silicon, to identify crystal-chemical similarities among these structures and to suggest other possible high-pressure silicate structure types.

Review of structures with six-coordinated silicon

There are fewer than 20 known structures with SiO_6 polyhedra (Table 1). These silicates can be divided conveniently into three groups. Above about 25 GPa, corresponding to the earth's lower mantle, all silicates studied to date are observed to transform to one of seven dense structures in which all Si is six-coordinated. These structures - rutile, perovskite, ilmenite, hollandite, calcium ferrite, pyrochlore and K_2NiF_4 - are well known room-pressure topologies for transition-metal oxides. In the high-pressure silicate

Table 1. *Compositions and calculated densities of silcates with* SiO_6 *octahedra*

Composition	Mineral name	Structure type	ρ_0 calc* ($g\ cm^{-3}$)
(*a*) High-pressure phases with SiO_6 groups only			
SiO_2	Stishovite	Rutile	4·29
$CaSiO_3$	-	Cubic perovskite	4·25
$MgSiO_3$	-	Ortho perovskite	4·10
$MgSiO_3$	-	Ilmenite	3·81
$ZnSiO_3$	-	Ilmenite	5·25
$KAlSi_3O_8$	-	Hollandite	3·91
$BaAl_2Si_2O_8$	-	Hollandite	5·3
$CaAl_2Si_2O_8$	-	Hollandite	3·9
$NaAlSiO_4$	-	Calcium ferrite	3·91
$Sc_2Si_2O_7$	-	Pyrochlore	4·28
$In_2Si_2O_7$	-	Pyrochlore	6·34
Ca_2SiO_4	-	K_2NiF_4	3·56
(*b*) High-pressure phases with $SiO_6 + SiO_4$ groups			
$MgSiO_3$	Majorite	Garnet	3·51
$MnSiO_3$	-	Garnet	4·32
$Na(Mg_{0.5}Si_{0.5})Si_2O_6$	-	Pyroxene	3·28
$K_2Si_4O_9$	-	Wadeite	3·09
$Mg_{14}Si_5O_{24}$	-	Anhydrous phase *B*	3·44
$Mg_{12}Si_4O_{19}(OH)_2$	-	Phase *B*	3·37
(*c*) Compounds with SiO_6 synthesized at room pressure			
SiP_2O_7-I	-	ZrP_2O_7	3·22
SiP_2O_7-III	-	-	3·05
SiP_2O_7-IV	-	-	3·11
$Si_5P_6O_{25}$	-	-	2·66
$(NH_4)_2SiP_4O_{13}$	-	-	2·37
$Ca_3(H_2O)_{12}[Si(OH)_6](CO_3)(SO_4)$	Thaumasite	-	1·87

* ρ_0 calc = density calculated from unit-cell parameters at room pressure and temperature.

isomorphs silicon occupies the octahedral transition-metal site, while other cations may adopt six or greater coordination.

At pressures between about 10 and 20 GPa some silicates form with mixed four and six coordination. These high-pressure phases, all of which may occur in the earth's transition zone, include silica-rich modifications of the well known garnet, pyroxene and wadeite structures, as well as complex new magnesium-bearing phases designated 'phase *B*' and 'anhydrous phase *B*'.

The third group of $^{[VI]}$Si silicates, including a variety of silicon phosphates, is distinguished by relatively open framework structures with corner sharing between silicon octahedra and other polyhedra of electronegative cations, notably $^{[IV]}$P. We describe each of these structures in the following section.

High-pressure silicates with all $^{[VI]}$Si

The stishovite structure. Stishovite, the form of SiO_2 synthesized above 10 GPa, is believed to be the stable form of free silica throughout most of the earth's volume. In addition to its assumed role in mantle mineralogy, stishovite has elicited considerable interest as a product of the transient high-pressure high-temperature environments of meteorite impacts (Chao, Fahey, Littler & Milton, 1962). The discovery

Table 2. *The* SiO_2 *stishovite structure*

Tetragonal, $P4_2/mnm$ (D_{4h}^{14}), $Z = 2$, $a = b = 4{\cdot}18$, $c = 2{\cdot}67$ Å, $V = 46{\cdot}6$ Å^3.

	Site	Symmetry	x	y	z
Si	2(*a*)	*mmm*	0	0	0
O	4(*f*)	*mm*	0·306	x	0

of stishovite grains in sediments near the Cretaceous-Tertiary boundary layer (McHone, Nieman & Lewis, 1989) has provided support for the hypothesis that a large impact, rather than volcanism, led to a mass extinction approximately 65 million years ago.

Stishovite has the simple rutile (TiO_2) structure (Table 2; Fig. 3), with edge-linked chains of SiO_6 octahedra that extend parallel to the c axis and octahedra corner linked to four adjacent chains. Two symmetrically distinct atoms - Si at (0, 0, 0) and O at (x, x, 0) with x approximately 0·3 - define the structure in space group $P4_2/mnm$.

The first stishovite structure refinements were obtained by powder diffraction on small synthetic samples (Stishov & Belov, 1962; Preisinger, 1962; Baur & Khan, 1971). A much improved refinement was presented by Sinclair & Ringwood (1978), who synthesized single crystals up to several hundred micrometres in diameter. Subsequent single-crystal structure studies by Hill, Newton & Gibbs (1983) under room conditions and by Sugiyama, Endo & Koto (1987) and Ross *et al.* (1990) at high pressure, amplify the earlier work (Table 3).

The silicate perovskite structure. Synthesis and structural description of silicate perovskites ($CaTiO_3$) have posed a significant challenge to earth scientists since Ringwood (1962, 1966) originally suggested the existence of perovskite forms of $MgSiO_3$ and $CaSiO_3$. High-pressure transformations from pyroxene and garnet structures to perovskite in the analogous systems $Ca(Ge,Si)O_3$ and $Ca(Ti,Si)O_3$ (Marezio, Remeika & Jayaraman, 1966; Ringwood & Major, 1967*a*, 1971; Reid & Ringwood, 1975) supported this hypothesis. Pure silicate perovskites were first produced at the Australian National University (Liu, 1974, 1975*a*,*b*, 1976*a*,*b*,*c*; Liu & Ringwood, 1975) and results were quickly duplicated in Japan and the United States (Sawamoto, 1977; Ito, 1977; Ito & Matsui, 1977, 1978, 1979; Mao, Yagi & Bell, 1977). These workers demonstrated that above pressures of about 27 GPa many silicates transform to the perovskite structure, in which silicon octahedra form a three-dimensional corner-linked network, while larger R cations fill positions with oxygen coordination of eight or greater. By the late 1970s many earth scientists were persuaded that the earth's 670 km seismic discontinuity, which divides the transition zone from the lower mantle, coincides with a perovskite phase-transition boundary, and that perovskite of approximate composition $(Mg_{0.9}Fe_{0.1})SiO_3$ is a

Table 3. *Stishovite structure refinements*

Distances are given in Å and angles in °.

	(1)	(2)	(3)	(4)
a	4·1772 (7)*	4·1773 (1)	4·1797 (2)	4·1801 (6)
c	2·6651 (4)	2·6655 (1)	2·6669 (1)	2·6678 (6)
x_O	0·3062 (2)	0·30608 (6)	0·30613 (7)	0·3067 (3)
Si–O [4]	1·7568 (5)	1·7572 (1)	1·7582 (2)	1·7564 (6)
Si–O [2]	1·8089 (10)	1·8087 (2)	1·8095 (3)	1·8130 (10)
Mean Si–O	1·774	1·774	1·775	1·775
O–Si–O	81·34 (5)	81·34 (1)	81·35 (2)	81·17 (5)
Octahedral volume (Å^3)†	7·359 (4)	7·361 (1)	7·373 (1)	7·369 (6)
Quadratic elongation†	1·0081 (3)	1·0081 (1)	1·0080 (1)	1·0084 (2)
Angle variance†	27·3	27·3	27·3	28·4

References: (1) Sinclair & Ringwood (1978), $R = 0{\cdot}015$; (2) Hill *et al.* (1983), $R = 0{\cdot}012$; (3) Sugiyama *et al.* (1987), $R = 0{\cdot}015$; (4) Ross, Shu *et al.* (1990), data collected on crystal in high-pressure cell, $R = 0{\cdot}014$.

* Parenthesized figures represent e.s.d.'s.

† Octahedral volume calculated with *VOLCAL* (Hazen & Finger, 1982). Quadratic elongation and angle variance are as described by Robinson, Gibbs & Ribbe (1971).

Table 4. *The cubic (a) and orthorhombic (b) silicate perovskite structures*

(*a*) $CaSiO_3$, cubic, $Pm\bar{3}m$ (O_h^1), $Z = 1$, $a = b = c =$ 3·567 (1) Å, $V = 45{\cdot}37$ (8) Å^3*

	Site	Symmetry	x	y	z
Si	1(*a*)	$m3m$	0	0	0
Ca	1(*b*)	$m3m$	$\frac{1}{2}$	$\frac{1}{2}$	$\frac{1}{2}$
O	3(*d*)	$4/mmm$	$\frac{1}{2}$	0	0

(*b*) $(Mg,Fe)SiO_3$, orthorhombic, $Pbnm$ (D_{2h}^{16}), $Z = 4$, $a = 4{\cdot}78$, $b = 4{\cdot}93$, $c = 6{\cdot}90$ Å, $V = 162{\cdot}4$ Å^3

	Site	Symmetry	x	y	z
Mg	4(*c*)	m	0·51	0·56	$\frac{1}{4}$
Si	4(*b*)	$\bar{1}$	$\frac{1}{2}$	0	$\frac{1}{2}$
O1	4(*c*)	m	0·10	0·47	$\frac{1}{4}$
O2	8(*d*)	1	0·20	0·20	0·55

* From Mao *et al.* (1989).

dominant lower mantle mineral (Anderson, 1976; Liu, 1977*a*, 1979; Yagi, Mao & Bell, 1978).

The simplest perovskite variant is the cubic form, represented by $CaSiO_3$, which is stable above about 15 GPa (Table 4*a*; Fig. 4*a*). This phase, first synthesized by Liu & Ringwood (1975), has a structure that is completely specified by the cubic cell edge, a, because all atoms are in invariant special positions. The Si- and O-atom positions, for example, are (0, 0, 0) and (1/2, 0, 0), respectively, so the Si–O distance of the regular silicon octahedron is $a/2$. Similarly, the octahedral volume is $a^3/6$. Calcium silicate perovskite cannot be quenched metastably to room pressure; samples invariably transform to glass upon release of pressure. Nevertheless, equation-of-state measurements of $CaSiO_3$ by Mao, Chen, Hemley, Jephcoat & Wu (1989) to 134 GPa define the structure as a function of pressure and allow reasonable extrapolation to room-pressure values (Table 4*a*).

The corner-linked silicate perovskite framework will tilt to accommodate divalent cations smaller than Ca. Thus, the structure of $(Mg,Fe)SiO_3$, widely thought to be the earth's most abundant mineral, is orthorhombic (Table 4*b*; Fig. 4*b*). Silicon occupies near-regular octahedral coordination, while magnesium is in a larger site with eight nearest-neighbor O atoms. Orthorhombic cell parameters possess a $2\sqrt{2} \times 2\sqrt{2} \times 2$ relationship to the simple cubic axes. Initial studies of this structure were performed by Yagi, Mao & Bell (1978, 1982) and Ito & Matsui (1978) on powders. Recent synthesis by Ito & Weidner (1986) of single crystals has led to much more precise structure refinements under room conditions (Horiuchi, Ito & Weidner, 1987) and at high pressure (Kudoh, Ito & Takeda, 1987; Ross & Hazen, 1990), as recorded in Table 5.

All silicate perovskite structure studies based on X-ray diffraction indicate complete ordering of Si and the divalent cations in the octahedral sites and the larger sites, respectively. Recently, however, Jackson, Knittle, Brown & Jeanloz (1987) examined a polycrystalline iron-bearing silicate perovskite of approximate composition $(Mg_{0{\cdot}9}Fe_{0{\cdot}1})SiO_3$ with EXAFS. Observation of significant $^{[VI]}$Fe led them to propose that some Si enters the eight-coordinated larger site. Single-crystal studies by Kudoh, Prewitt, Finger, Darovskikh & Ito (1990) and powder diffraction data by Parise, Wang, Yeganeh-Haeri, Cox & Fei (1990) on iron-bearing samples do not support this interpretation – they find all Fe in the larger site, as would be expected from crystal-chemical arguments. Kirkpatrick, Howell, Phillips, Cong, Ito & Navrotsky (1991) came to the same conclusion based on ^{29}Si NMR spectroscopy of $MgSiO_3$ perovskite.

The ilmenite structure. The ilmenite ($FeTiO_3$) and corundum (α-Al_2O_3) structures have long been recognized as likely candidates for high-pressure silicates in which all cations assume octahedral coordi-

Table 5. $MgSiO_3$ *perovskite structure refinements*

Distances are given in Å and angles in °.

	(1)	(2)	(3)	(4)	(5)
a	4·7754 (3)	4·780 (1)	4·7787 (4)	4·745 (2)	4·772 (2)
b	4·9292 (4)	4·933 (1)	4·9313 (4)	4·907 (1)	4·927 (1)
c	6·8969 (5)	6·902 (1)	6·9083 (8)	6·853 (2)	6·8977 (1)
x_{Mg}	0·524 (6)	0·524 (7)	0·5141 (1)	0·5169 (14)	1·5131 (7)
y_{Mg}	0·561 (5)	0·563 (5)	0·5560 (1)	0·5573 (10)	0·5563 (4)
x_{O1}	0·096 (8)	0·096 (10)	0·1028 (2)	0·1087 (24)	0·1031 (12)
y_{O1}	0·468 (12)	0·477 (11)	0·4660 (2)	0·4659 (22)	0·4654 (9)
x_{O2}	0·201 (9)	0·196 (7)	0·1961 (1)	0·1965 (15)	0·1953 (7)
y_{O2}	0·205 (8)	0·209 (7)	0·2014 (2)	0·2037 (15)	0·2010 (6)
z_{O2}	0·558 (4)	0·556 (4)	0·5531 (1)	0·5558 (7)	0·5510 (4)
Si-O1 [2]	1·79 (1)	1·79 (1)	1·8005 (3)	1·797 (3)	1·801 (1)
Si-O2 [2]	1·79 (1)	1·76 (3)	1·7827 (7)	1·794 (7)	1·795 (4)
Si-O2 [2]	1·79 (1)	1·82 (3)	1·7960 (7)	1·769 (7)	1·779 (3)
Mean Si-O	1·79	1·79	1·793	1·787	1·792
O1-Si-O2	86·5	87·9	88·66 (5)	88·6 (4)	88·2 (2)
O1-Si-O2	89·6	88·6	88·49 (5)	88·8 (4)	89·0 (2)
O2-Si-O2	88·9	89·4	89·43 (3)	89·4 (3)	89·59 (5)
Octahedral volume (Å^3)*	7·65 (17)	7·63 (15)	7·702 (3)	7·60 (3)	7·657 (14)
Quadratic elongation	1·002 (15)	1·001 (15)	1·0005 (3)	1·00	1·005 (16)
Angle variance	6·3	2·3	1·6	1·4	1·7

References: (1) Ito & Matsui (1978), based on powder XRD; (2) Yagi *et al.* (1978), based on powder XRD, $R = 0·10$; (3) Horiuchi *et al.* (1987), single crystal in air, $R = 0·035$; (4) Kudoh *et al.* (1987), single crystal at 4·0 GPa, $R = 0·079$; (5) Ross & Hazen (1990), single crystal in pressure cell at room pressure, $R = 0·042$.

* See Table 3.

Table 6. *Refinement of the* $MgSiO_3$ *ilmenite structure, from Horiuchi et al.* (1982), $R = 0·049$

Rhombohedral, $R\bar{3}$ (C_{3i}^2), $Z = 6$, $a = 4·7284$ (4), $c = 13·5591$ (16) Å, $V = 262·5$ Å^3. Distances are given in Å and angles in °.

	Site	Symmetry	x	y	z
Mg	2(g)	3	0	0	0·35970 (12)
Si	2(g)	3	0	0	0·15768 (10)
O	6(i)	1	0·3214 (5)	0·0361 (4)	0·24077 (11)

Si-O [3]	1·830 (2)	Mg-O [3]	2·163 (2)
Si-O [3]	1·768 (2)	Mg-O [3]	1·990 (2)
Mean Si-O	1·799	Mean Mg-O	2·077
O-Si-O	80·8 (1)	O-Mg-O	70·5 (1)
O-Si-O	86·1 (1)	O-Mg-O	90·1 (1)
O-Si-O	96·4 (1)	O-Mg-O	94·5 (1)
O-Si-O	97·2 (1)	O-Mg-O	101·2 (1)
Octahedral volume (Å^3)*	7·59 (1)	Octahedral volume (Å^3)	11·30 (1)
Quadratic elongation	1·015	Quadratic elongation	1·04 (1)
Angle variance	52·8	Angle variance	141·6

* See Table 3.

nation [J. B. Thompson in Birch (1952)]. (The two structures differ only in the lack of ordered cations in corundum.) Ringwood & Seabrook (1962) demonstrated such a transformation in the germanate analog, $MgGeO_3$, and other high-pressure germanate isomorphs were soon identified. The silicate end member $MgSiO_3$ was subsequently produced by Kawai, Tachimori & Ito (1974) and this material was identified by Ito & Matsui (1974) as having the ilmenite ($R\bar{3}$) structure, in which silicon and magnesium must be at least partially ordered (Table 6; Fig. 5).

Horiuchi, Hirano, Ito & Matsui (1982) synthesized single crystals of $MgSiO_3$ ilmenite and documented details of the crystal structure. Silicon and magnesium appear to be almost completely ordered in the two symmetrically distinct cation positions (Table 6). Silicate ilmenites are unique in that each silicon octahedron shares a face with an adjacent magnesium octahedron - no other known silicate structure displays face sharing between a silicon polyhedron and another tetrahedron or octahedron. Magnesium-silicon ordering may be facilitated by this feature, for only in a completely ordered silicate ilmenite can face sharing between two silicon octahedra be avoided.

The stability of silicate ilmenites is rather restricted, in terms of both pressure and composition. Pressures above 20 GPa are required to synthesize the $MgSiO_3$

Table 7. *Refinement of the* $KAlSi_3O_8$ *hollandite structure, from Yamada et al.* (1984), $R = 0{\cdot}137$

Tetragonal, $I4/m$ (C_{4h}^5), $Z = 2$, $a = 9{\cdot}3244\,(4)$, $c = 2{\cdot}7227\,(3)$ Å, $V = 236{\cdot}7$ Å^3. Distances are given in Å and angles in °.

	Site	Symmetry	x	y	z
K	2(*b*)	4/*m*	0	0	$\frac{1}{2}$
M($\frac{1}{4}$Al + $\frac{3}{4}$Si)	8(*h*)	*m*	0·348 (4)	0·170 (3)	0
O1	8(*h*)	*m*	0·143 (5)	0·219 (5)	0
O2	8(*h*)	*m*	0·541 (6)	0·162 (6)	0

M-O1	1·97 (4)	O1-*M*-O2	79 (2)
M-O1 [2]	1·71 (1)	O1-*M*-O2	89 (3)
M-O2	1·80 (4)	O1-*M*-O2	96 (2)
M-O2 [2]	1·82 (4)	O2-*M*-O2	91 (3)
Mean *M*-O	1·81	O2-*M*-O2	97 (3)
O1-*M*-O1	85 (3)	Octahedral volume (Å^3)*	7·62 (23)
O1-*M*-O1	106 (3)	Quadratic elongation	1·02 (4)
		Angle variance	60·5

* See Table 3.

Table 8. *Refinement of the* $NaAlSiO_4$ *calcium ferrite structure, from Yamada et al.* (1983), $R = 0{\cdot}039$, *with revised and corrected atomic coordinates*

Orthorhombic, *Pbnm* (D_{2h}^{16}), $Z = 4$, $a = 10{\cdot}1546\,(8)$, $b = 8{\cdot}6642\,(8)$, $c = 2{\cdot}7385\,(4)$ Å, $V = 240{\cdot}93\,(3)$ Å^3.

	Site	Symmetry	x†	y	z
Na	4(*c*)	*m*	0·339 (3)	0·236 (3)	$\frac{1}{4}$
*M*1*	4(*c*)	*m*	0·890 (3)	0·577 (4)	$\frac{1}{4}$
*M*2*	4(*c*)	*m*	0·398 (3)	0·556 (3)	$\frac{1}{4}$
O1	4(*c*)	*m*	0·635 (5)	0·303 (5)	$\frac{1}{4}$
O2	4(*c*)	*m*	0·982 (5)	0·388 (5)	$\frac{1}{4}$
O3	4(*c*)	*m*	0·216 †	0·479 †	$\frac{1}{4}$
O4	4(*c*)	*m*	0·430 (4)	0·438 (6)	$\frac{3}{4}$‡

* Octahedral sites treated as disordered Al + Si.

† Published coordinates are approximately correct, but they yield several unreasonably short octahedral bond distances. Refined O3 coordinates, 0·201 (5) and 0·461 (5), have been replaced in this table for consistency.

‡ z coordinate of O4 was incorrectly given as 1/4 in the original paper.

phase, but above about 25 GPa perovskite forms instead (Fei, Saxena & Navrotsky, 1990; see Fig. 2). Addition of more than a few atom percent iron for magnesium stabilizes the perovskite form at the expense of ilmenite; 10% iron completely eliminates the ilmenite field. Of the other common divalent cations, only zinc has been found to form a stable silicate ilmenite - $ZnSiO_3$ (Ito & Matsui, 1974; Liu, 1977*b*).

The hollandite structure. Feldspars, including $KAlSi_3O_8$, $NaAlSi_3O_8$ and $CaAl_2Si_2O_8$, are the most abundant minerals in the earth's crust. Accordingly, a number of researchers have examined high-pressure phase relations for these minerals (Kume, Matsumoto & Koizumi, 1966; Ringwood, Reid & Wadsley, 1967; Reid & Ringwood, 1969; Kinomura, Kume & Koizumi, 1975; Liu, 1978*a*,*b*). All of these investigators concluded that feldspars ultimately transform to the hollandite ($BaMn_8O_{16}$) structure at pressures above about 10 GPa. Hollandite-type silicates have thus been proposed as a primary repository for alkalis in the earth's mantle.

The ideal hollandite structure is tetragonal, $I4/m$, with double chains of edge-sharing (Si,Al) octahedra (Fig. 6; Table 7). Large alkali or akaline-earth cations occupy positions along large channels that run parallel to c. The structure of $KAlSi_3O_8$ hollandite was refined from powder diffraction data by Yamada, Matsui & Ito (1984). They detected no deviations from tetragonal symmetry and so assumed complete disorder of aluminium and silicon on the one symmetrically distinct octahedral site. Natural hollandites, however, are typically monoclinic (pseudo-tetragonal) owing to ordering of Mn^{3+} and Mn^{4+} or other octahedral cations, as well as distortion of the channels. Single crystals of $KAlSi_3O_8$ hollandite have recently been synthesized at the Mineral Physics Institute, State University of New York (Jaidong Ko, personal communication) and these samples may reveal if aluminium-silicon ordering lowers the apparent tetragonal symmetry.

A number of other silicate hollandites have been synthesized but not fully characterized by X-ray diffraction. Reid & Ringwood (1969) made hollandites with compositions approximating $SrAl_2Si_2O_8$ and $BaAl_2Si_2O_8$ (though reported alkaline-earth contents are significantly less than 1·0), while Madon, Castex & Peyronneau (1989) described synthesis of $(Ca_{0.5}Mg_{0.5})Al_2Si_2O_8$ hollandite. Given the 1 : 1 ratio of aluminium to silicon in these samples, ordering of Al and Si into symmetrically distinct octahedra is possible, though structure-energy calculations by Post & Burnham (1986) suggest that octahedral cations are disordered in most hollandites. This proposition is supported by Vicat, Fanchan, Strobel & Qui's (1986) ordering studies of synthetic hollandite ($K_{1.33}Mn^{4+}_{6.67}Mn^{3+}_{1.33}O_{16}$), which displays diffuse diffraction effects characteristic of some short-range order, but long-range disorder of Mn^{4+} and Mn^{3+}.

The calcium ferrite structure. High-pressure studies of $NaAlGeO_4$ (Ringwood & Major, 1967*a*; Reid, Wadsley & Ringwood, 1967) and $NaAlSiO_4$ (Liu, 1977*c*, 1978*a*; Yamada, Matsui & Ito, 1983) revealed that these compounds adopt the orthorhombic calcium ferrite ($CaFe_2O_4$) structure in which all Si and Al are in octahedral coordination. Yamada *et al.* (1983), who synthesized $NaAlSiO_4$ at pressures above 24 GPa, used X-ray diffraction to identify their polycrystalline product and propose atomic coordinates. The basic topology of the high-pressure $NaAlSiO_4$ structure is thus well established (Fig. 7; Table 8). Bond distances calculated from their refined coordinates, however, yield unreasonably short cation-oxygen distances, so details of the structure remain in doubt.

The calcium ferrite structure bears a close relationship to hollandite (Yamada *et al.*, 1983). Both struc-

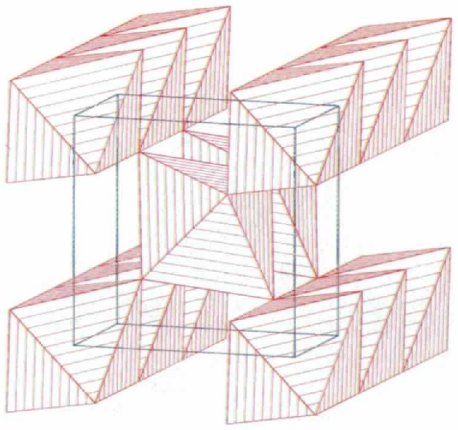

Fig. 3. The SiO_2 stishovite structure, after Smyth & Bish (1988).

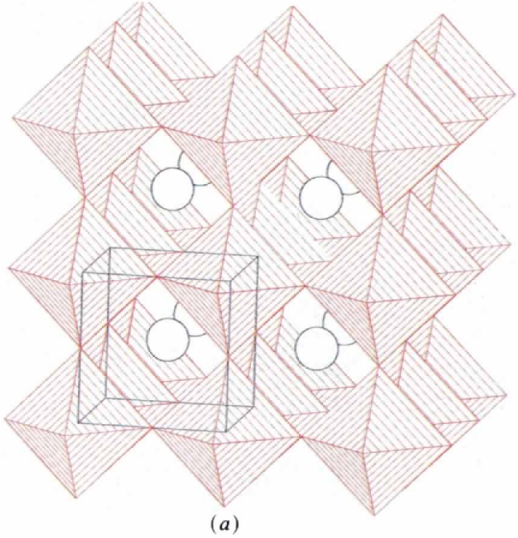

(*a*)

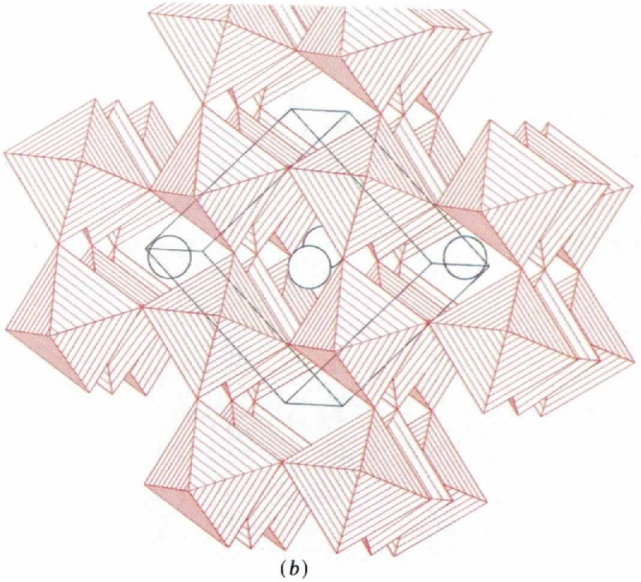

(*b*)

Fig. 4. The cubic (*a*) and orthorhombic (*b*) silicate perovskite structures, after Hazen (1988).

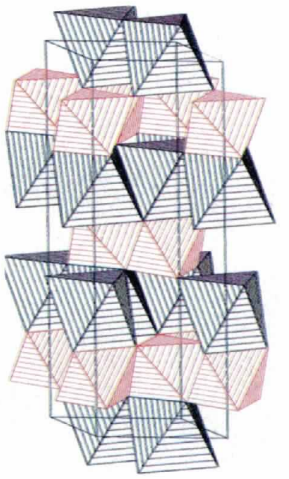

Fig. 5. The $MgSiO_3$ ilmenite structure, based on the refinement of Horiuchi *et al.* (1982).

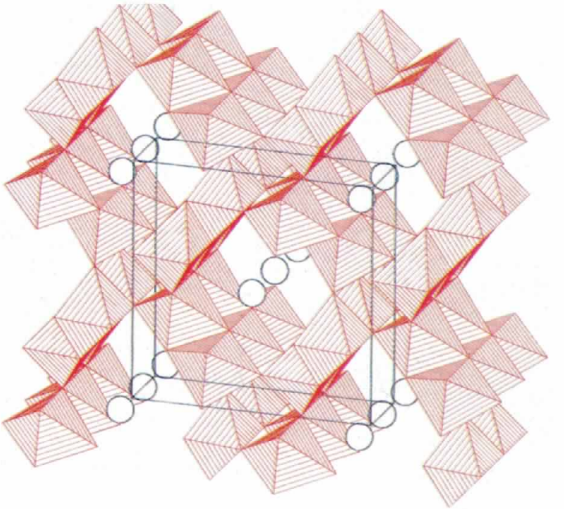

Fig. 6. The $KAlSi_3O_8$ hollandite structure, based on the refinement of Yamada *et al.* (1984).

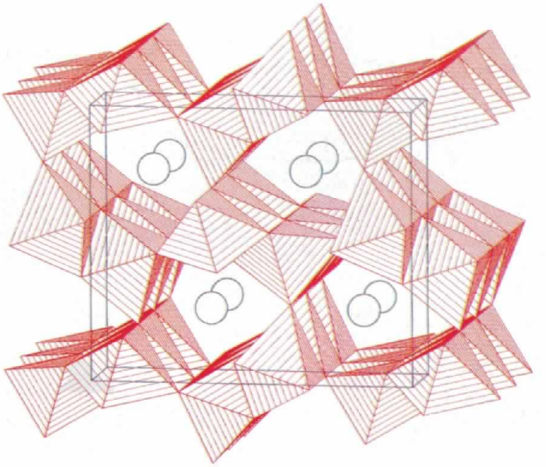

Fig. 7. The $NaAlSiO_4$ calcium ferrite structure, modified from the refinement of Yamada *et al.* (1983).

[*To face p.* 566

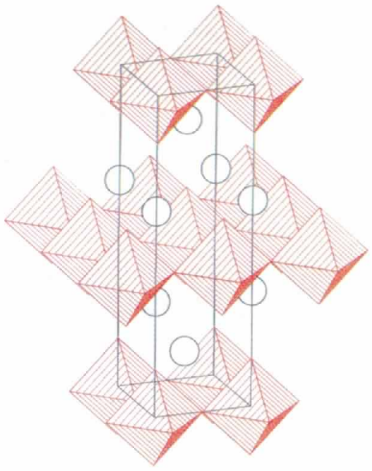

Fig. 8. The K_2NiF_4 structure, after Jorgensen (1987).

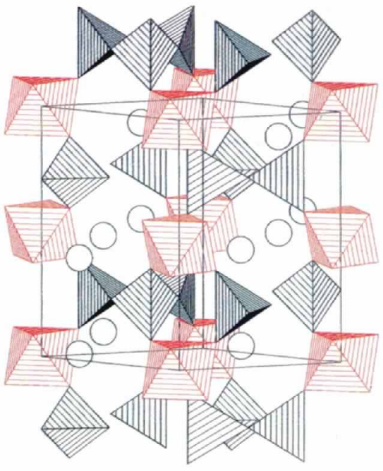

Fig. 11. The structure of $K_2{}^{[VI]}Si^{[IV]}Si_3O_9$, after Swanson & Prewitt (1983).

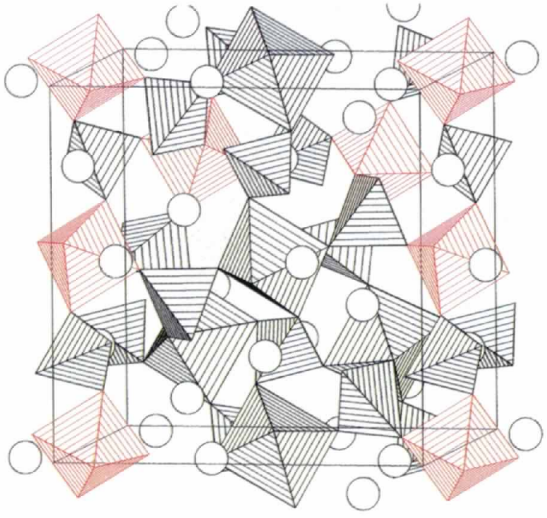

Fig. 9. The structure of $MgSiO_3$ garnet, after Smyth & Bish (1988).

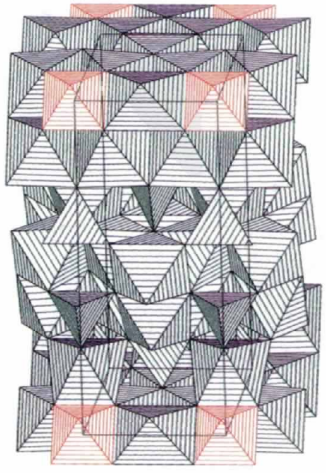

Fig. 12. The structure of anhydrous phase *B*, from Finger *et al.* (1989).

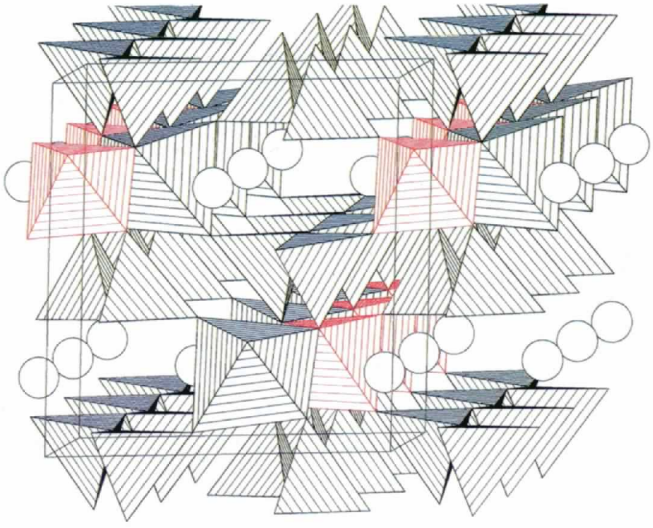

Fig. 10. The structure of $Na(Mg_{0.5}Si_{0.5})Si_2O_6$ pyroxene, from Angel *et al.* (1988).

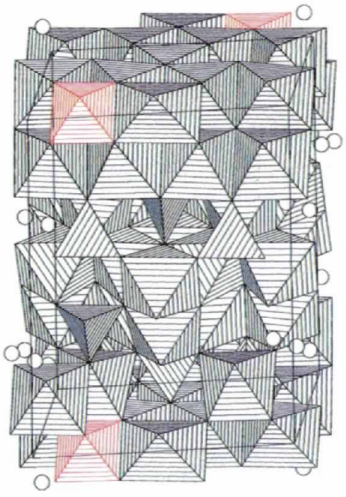

Fig. 13. The structure of $Mg_{12}Si_4O_{19}(OH)_2$ (phase *B*), from Finger *et al.* (1989).

Table 9. *Refinement of silicate pyrochlore structures, from Reid et al.* (1977), $R = 0{\cdot}031$ *for* $Sc_2Si_2O_7$ *and* $R = 0{\cdot}015$ *for* $In_2Si_2O_7$

Cubic, $Fd\bar{3}m$ (O_h^7), $Z = 8$. $Sc_2Si_2O_7$: $a = 9{\cdot}287\,(3)$ Å, $V = 800{\cdot}98\,(1)$ Å^3. $In_2Si_2O_7$: $a = 9{\cdot}413\,(3)$ Å, $V = 834{\cdot}03\,(1)$ Å^3. Distances are given in Å and angles in °.

	Site	Symmetry	x	y	z
Sc, In	16(*c*)	$\bar{3}m$	0	0	0
Si	16(*d*)	$3m$	$\frac{1}{2}$	$\frac{1}{2}$	$\frac{1}{2}$
O1	8(*a*)	$\bar{4}3m$	$\frac{1}{8}$	$\frac{1}{8}$	$\frac{1}{8}$
O2	48(*f*)	*mm*	Sc: 0·4313 (21)	$\frac{1}{8}$	$\frac{1}{8}$
			In: 0·4272 (15)		

	$Sc_2Si_2O_7$	$In_2Si_2O_7$
Si-O2 [6]	1·761 (7)	1·800 (5)
O2-Si-O2 [6]	92·5 (7)	94·0 (6)
O2-Si-O2 [6]	87·5 (7)	86·0 (6)
Octahedral volume (Å^3)*	7·26 (3)	7·71 (2)
Quadratic elongation	1·002 (9)	1·005 (7)
Angle variance	6·7	17·8

* See Table 3.

tures consist of double octahedral chains which are joined to form 'tunnels' parallel to **c** that accommodate the alkali or alkaline-earth cations. In hollandite four double chains form square tunnels, whereas in calcium ferrite four chains define triangular tunnels.

The pyrochlore $[(Na,Ca)_2(Nb,Ta)_2O_6(OH,F)]$ *structure.* Thortveitite, $Sc_2Si_2O_7$, contains Si_2O_7 groups and Sc in distorted octahedral coordination. The structure is unusual in that the Si–O–Si linkage is constrained to be collinear because the O atom lies on a center of inversion. Reid, Li & Ringwood (1977) studied high-pressure transformations of $Sc_2Si_2O_7$ and its isomorph, $In_2Si_2O_7$, from the thortveitite structure to the pyrochlore structure at 12 GPa and 1273 K. They report structures based on powder X-ray diffraction data from these two high-pressure compounds.

The cubic pyrochlore structure (space group $Fd\bar{3}m$) contains four independent atoms with only one variable positional parameter, the x coordinate of O2 (Table 9). It features silicon in an octahedral framework corner-linked by O2, with scandium in distorted cubic eight coordination corner-linked by O1. The increase in coordination number of both cations, from 4 and 6 in thortveitite to 6 and 8 in pyrochlore, leads to a significant density increase, from 3·30 g cm^{-3} in thortveitite to 4·28 g cm^{-3} in the high-pressure phase.

The K_2NiF_4 *structure.* The potassium nickel fluoride structure, in which K and Ni are nine- and six-coordinated respectively, is well known among transition-metal oxides such as Sr_2TiO_4. Reid & Ringwood (1970) proposed K_2NiF_4 as a possible high-pressure silicate structure following their synthesis of Ca_2GeO_4. Liu (1978*b*) synthesized a high-pressure polymorph of Ca_2SiO_4 at between 22 and 26 GPa and

Table 10. *The structure of* K_2NiF_4*-type* Ca_2SiO_4, *after Liu* (1978*b*)

Tetragonal, $I4/mmm$ (D_{4h}^{17}), $Z = 2$, $a = 3{\cdot}564\,(2)$, $c = 11{\cdot}66\,(1)$ Å, $V = 148{\cdot}1\,(1)$ Å^3. Distances are given in Å and angles in °.

	Site	Symmetry	x	y	z*
Ca	4(*e*)	4*mm*	0	0	~0·36
Si	2(*a*)	4/*mmm*	0	0	0
O1	4(*c*)	*mmm*	0	$\frac{1}{2}$	0
O2	4(*e*)	4*mm*	0	0	~0·15

Si-O1 [4]	1·782 (1)	O1-Si-O1 [4]	90
Si-O2 [2]	~1·78	O1-Si-O2 [8]	90

* Fractional coordinates not reported.

1273 K and recognized the distinctive tetragonal cell [$a = 3{\cdot}564\,(3)$, $c = 11{\cdot}66\,(1)$ Å] as characteristic of the K_2NiF_4 structure. 25 powder diffraction lines consistent with this unit cell were recorded by Liu, although structural details of the high-pressure calcium silicate were not provided.

The aristotype structure with K_2NiF_4 topology (Table 10; Fig. 8) is tetragonal, space group $I4/mmm$, with four atoms in the asymmetric unit and only two variable positional parameters. Octahedrally coordinated Ni (or Si) at the origin is coordinated to four F1 (or O1) at $(0, \frac{1}{2}, 0)$ and two F2 (or O2) at $(0, 0, z)$. Four Ni–F (or Si–O1) bond distances are exactly $a/2$ and all adjacent F–Ni–F (or O–Si–O) angles are 90°.

Slight distortions of the $I4/mmm$ structure lead to a number of subgroups of lower-symmetry variants (Hazen, 1990). These topologically identical structures have received much attention recently because the first copper oxide superconductor, $(La,Ba)_2CuO_4$, adopts the K_2NiF_4 topology. Additional studies of Ca_2SiO_4 will be required to resolve the exact nature of this high-pressure phase.

High-pressure silicates with mixed $^{[IV]}$Si *and* $^{[VI]}$Si

The garnet structure. Garnets are common crustal silicates of the general formula $^{[VIII]}A_3^{2+}{}^{[VI]}B_2^{3+}$-$^{[IV]}Si_3^{4+}O_{12}$, where eight-coordinated A is commonly Mg, Fe, Mn or Ca and six-coordinated B is usually Fe, Al or Cr. The structure may be viewed as a corner-linked framework of alternating Si^{4+} tetrahedra and trivalent octahedra. This framework defines eight-coordinated sites that accommodate divalent cations (Fig. 9). The ideal garnet structure is cubic (space group $Ia\bar{3}d$), with only four symmetry-independent atoms: A, B, Si and O.

Ringwood & Major (1967*a*) and Prewitt & Sleight (1969) demonstrated that germanate garnets of compositions $^{[VIII]}Cd_3{}^{[VI]}(CdGe)^{[IV]}Ge_3O_{12}$ and $^{[VIII]}Ca_3{}^{[VI]}(CaGe)^{[IV]}Ge_3O_{12}$ form because germanium plus a divalent cation can substitute for the trivalent B cation. These garnets are topologically identical to the cubic aristotype, but ordering of octahedral B cations yields a garnet of symmetry

Table 11. *Refinement of the structure of* $MgSiO_3$ *garnet, from Angel et al.* (1989), $R = 0{\cdot}043$

Tetragonal, $I4_1/a$ (C_{4h}^6), $Z = 32$, $a = 11{\cdot}501\ (1)$, $c = 11{\cdot}480\ (2)$ Å, $V = 1518{\cdot}5$ Å^3. Distances are given in Å and angles in °.

	Occupancy	Site*	Symmetry	x	y	z
*D*1	Mg	16(*f*)	1	0·1253 (4)	0·0112 (4)	0·2587 (3)
*D*2	Mg	8(*e*)	2	0	$\frac{1}{4}$	0·6258 (6)
Oct. 1	0·8Si + 0·2Mg	8(*c*)	$\bar{1}$	0	0	$\frac{1}{2}$
Oct. 2	0·2Si + 0·8Mg	8(*d*)	$\bar{1}$	0	0	0
*T*1	Si	4(*b*)	$\bar{4}$	0	$\frac{1}{4}$	$\frac{3}{8}$
*T*2	Si	4(*a*)	$\bar{4}$	0	$\frac{1}{4}$	$\frac{1}{8}$
*T*3	Si	16(*f*)	1	0·1249 (3)	0·0065 (3)	0·7544 (3)
O1	O	16(*f*)	1	0·0282 (6)	0·0550 (6)	0·6633 (6)
O2	O	16(*f*)	1	0·0380 (6)	−0·0471 (6)	0·8562 (6)
O3	O	16(*f*)	1	0·2195 (7)	0·1023 (6)	0·8021 (6)
O4	O	16(*f*)	1	0·2150 (6)	−0·0894 (6)	0·7000 (6)
O5	O	16(*f*)	1	−0·0588 (6)	0·1617 (6)	0·4680 (6)
O6	O	16(*f*)	1	−0·1040 (6)	0·2080 (6)	0·7851 (6)

Oct. 2-O2 [2]	1·792 (7)	Oct. 1-O1 [2]	2·004 (7)
Oct. 2-O3 [2]	1·836 (7)	Oct. 1-O4 [2]	1·976 (7)
Oct. 2-O6 [2]	1·793 (7)	Oct. 1-O5 [2]	2·012 (7)
Mean Oct. 2-O	1·807	Mean Oct. 1-O	1·997
O2-Oct. 2-O3	89·0 (3)	O1-Oct. 1-O4	86·8 (3)
O2-Oct. 2-O6	89·4 (3)	O1-Oct. 1-O5	86·2 (3)
O3-Oct. 2-O6	89·8 (3)	O4-Oct. 1-O5	85·8 (3)
Octahedral volume (Å^3)†	7·86 (3)	Octahedral volume (Å^3)	10·56 (4)
Quadratic elongation	1·000 (4)	Quadratic elongation	1·004 (4)
Angle variance	0·5	Angle variance	15·4

* Origin of atomic coordinates shifted by $\frac{1}{2}$, 0, 0 relative to standard origin at Wyckoff position 8(*c*), in conformity with previous descriptions of tetragonal garnets.

† See Table 3.

group lower than the $Ia\bar{3}d$ form. Ringwood & Major (1967*a*) were the first to synthesize a high-pressure silicate garnet, $MnSiO_3$, which Akimoto & Syono (1972) subsequently indexed as tetragonal. High-pressure silicate garnets thus incorporate silicon in both four and six coordination.

The significance of these synthetic samples has been enhanced by discovery of natural high-pressure garnets with $^{[VI]}$Si. Smith & Mason (1970) described a natural silica-rich garnet from the Coorara meteorite. The composition of this mineral, which they named majorite, is $^{[VIII]}(Mg_{2\cdot86}Na_{0\cdot10}\square_{0\cdot04})$-$^{[VI]}(Fe_{0\cdot97}Al_{0\cdot22}Cr_{0\cdot03}Si_{0\cdot78})^{[IV]}Si_3O_{12}$. Haggerty & Sautter (1990) recently discovered mantle-derived nodules with silica-rich garnet of composition of more than four Si atoms per 12 O atoms (as opposed to three Si in crustal garnets). These observations led the authors to propose that the nodules originated from a depth greater than 300 km – by far the deepest terrestrial samples thus identified.

Single crystals of $MnSiO_3$ garnet were first synthesized by Fujino, Momoi, Sawamoto & Kumazawa (1986), who determined the space group to be tetragonal ($I4_1/a$). Mn and Si atoms were found to be fully ordered in two symmetrically distinct octahedral sites (Table 11). At pressures above 15 GPa and temperatures greater than about 1973 K, $MgSiO_3$ forms the garnet $^{[VIII]}Mg_3^{[VI]}(MgSi)^{[IV]}Si_3O_{12}$ – the same composition as the silicate ilmenites and perovskites described above. Angel *et al.* (1989) synthesized single crystals of this phase and determined the crystal structure (Table 12). In that sample, octahedral Mg and Si were slightly disordered, yielding a site composition of $(Si_{0\cdot8}Mg_{0\cdot2})$.

The pyroxene structure. Pyroxenes, among the most common constituents of igneous and metamorphic rocks, typically have compositions $ASiO_3$, where A may consist entirely of divalent Mg, Fe and Ca or may contain a mixture of cations with +1, +2 and +3 valences. Angel, Gasparik, Ross, Finger, Prewitt & Hazen (1988) recently described an unusual high-pressure synthetic pyroxene with composition $Na^{[VI]}(Mg_{0\cdot5}Si_{0\cdot5})^{[IV]}Si_2O_6$. Silicon and magnesium form an ordered edge-sharing octahedral chain in this structure (Fig. 10; Table 13).

Angel *et al.* (1988) note that it is doubtful such a pyroxene plays a significant role in the earth's mantle, for its stability is limited to silica-rich compositions with an excess of sodium with respect to aluminium – a situation rarely encountered in nature.

The wadeite structure ($K_2^{[VI]}Si^{[IV]}Si_3O_9$). The wadeite ($K_2ZrSi_3O_9$) structure features Si_3O_9 three-tetrahedra corner-linked rings cross linked by Zr octahedra, forming a framework with hexagonal symmetry (space group $P6_3/m$). Potassium occupies large nine-coordinated cavities between adjacent three-member Si tetrahedral rings. Germanate isomorphs, including $K_2GeSi_3O_9$ (Reid *et al.*, 1967), $K_2Ge_4O_9$ (Voellenkle & Wittmann, 1971) and $(LiNa)Ge_4O_9$ (Voellenkle, Wittmann & Nowotny, 1969), pointed

Table 12. *Refinement of the structure of* $MnSiO_3$ *garnet, from Fujino et al.* (1986), $R = 0{\cdot}052$

Tetragonal, $I4_1/a$ (C_{4h}^6), $Z = 32$, $a = 11{\cdot}774\,(1)$, $c = 11{\cdot}636\,(2)$ Å, $V = 1613{\cdot}1$ Å^3. Distances are given in Å and angles in °.

	Occupancy	Site	Symmetry	x	y	z
*D*1	Mn	16(*f*)	1	0·1258 (1)	0·0079 (1)	0·2590 (1)
*D*2	Mn	8(*e*)	2	0	$\frac{1}{4}$	0·6235 (2)
Oct. 1	0·98Mn + 0·02Si	8(*c*)	$\bar{1}$	0	0	$\frac{1}{2}$
Oct. 2	0·98Si + 0·02Mn	8(*d*)	$\bar{1}$	0	0	0
*T*1	Si	4(*b*)	$\bar{4}$	0	$\frac{1}{4}$	$\frac{3}{8}$
*T*2	Si	4(*a*)	$\bar{4}$	0	$\frac{1}{4}$	$\frac{1}{8}$
*T*3	Si	16(*f*)	1	0·1262 (2)	0·0143 (1)	0·7597 (2)
O1	O	16(*f*)	1	0·0302 (4)	0·0617 (4)	0·6730 (4)
O2	O	16(*f*)	1	0·0465 (4)	−0·0411 (4)	0·8627 (4)
O3	O	16(*f*)	1	0·2224 (4)	0·1099 (4)	0·8064 (4)
O4	O	16(*f*)	1	0·2098 (4)	−0·0796 (4)	0·7039 (4)
O5	O	16(*f*)	1	−0·0649 (4)	0·1665 (4)	0·4654 (4)
O6	O	16(*f*)	1	−0·1034 (4)	0·2152 (4)	0·7858 (4)

Oct. 2-O2 [2]	1·757 (4)	Oct. 1-O1 [2]	2·170 (4)
Oct. 2-O3 [2]	1·805 (4)	Oct. 1-O4 [2]	2·130 (4)
Oct. 2-O6 [2]	1·823 (4)	Oct. 1-O5 [2]	2·142 (5)
Mean Oct. 2-O	1·795	Mean Oct. 1-O	2·147
O2-Oct. 2-O3	89·8 (2)	O1-Oct. 1-O4	85·8 (2)
O2-Oct. 2-O6	89·0 (2)	O1-Oct. 1-O5	89·7 (2)
O3-Oct. 2-O7	87·2 (2)	O4-Oct. 1-O5	85·1 (2)
Octahedral volume (Å^3)†	7·69 (2)	Octahedral volume (Å^3)	13·11 (3)
Quadratic elongation	1·001 (3)	Quadratic elongation	1·004 (3)
Angle variance	3·1	Angle variance	15·2

* Origin of atomic coordinates shifted by $\frac{1}{2}$, 0, 0 relative to standard origin of Wyckoff position 8(*c*), in conformity with previous descriptions of tetragonal garnets.

† See Table 3.

Table 13. *Refinement of the structure of* $Na(Mg_{0{\cdot}5}Si_{0{\cdot}5})Si_2O_6$ *pyroxene, from Angel et al.* (1988), $R = 0{\cdot}045$

Monoclinic, $P2/n$ (C_{2h}^2), $Z = 4$, $a = 9{\cdot}418\,(1)$, $b = 8{\cdot}647\,(1)$, $c = 5{\cdot}274\,(1)$ Å, $\beta = 108{\cdot}13\,(1)°$, $V = 408{\cdot}2$ Å^3. Distances are given in Å and angles in °.

	Occupancy	Site	Symmetry	x	y	z
*M*1*A*	Mg	2(*f*)	2	$\frac{3}{4}$	0·6549 (2)	$\frac{1}{4}$
*M*1*B*	Si	2(*e*)	2	$\frac{3}{4}$	0·8469 (2)	$\frac{3}{4}$
*M*2*A*	Na	2(*f*)	2	$\frac{3}{4}$	0·0513 (2)	$\frac{1}{4}$
*M*2*B*	Na	2(*e*)	2	$\frac{3}{4}$	0·4567 (3)	$\frac{3}{4}$
*T*1	Si	4(*g*)	1	0·0447 (1)	0·8486 (1)	0·2270 (2)
*T*2	Si	4(*g*)	1	0·0372 (1)	0·6652 (1)	0·7355 (2)
O1*A*	O	4(*g*)	1	0·8620 (3)	0·8443 (3)	0·1017 (4)
O1*B*	O	4(*g*)	1	0·8567 (3)	0·6934 (3)	0·6562 (5)
O2*A*	O	4(*g*)	1	0·1234 (3)	0·0146 (3)	0·3077 (5)
O2*B*	O	4(*g*)	1	0·0982 (3)	0·4950 (3)	0·7911 (5)
O3*A*	O	4(*g*)	1	0·1128 (3)	0·7665 (3)	0·0119 (5)
O3*B*	O	4(*g*)	1	0·0930 (3)	0·7527 (3)	0·5070 (5)

*M*1*B*-O1*A* [2]	1·826 (2)	*M*1*A*-O1*A*	2·219 (3)
*M*1*B*-O1*B* [2]	1·924 (2)	*M*1*A*-O1*B*	2·090 (2)
*M*1*B*-O2*A* [2]	1·782 (3)	*M*1*A*-O2*B*	1·991 (3)
Mean *M*1*B*-O	1·811	Mean *M*1*A*-O	2·100
O1*A*-*M*1*B*-O1*B*	84·7	O1*A*-*M*1*A*-O1*A*	84·8
O1*A*-*M*1*B*-O1*B*	94·2	O1*A*-*M*1*A*-O1*B*	96·6
O1*A*-*M*1*B*-O2*A*	92·3	O1*A*-*M*1*A*-O1*B*	69·6
O1*A*-*M*1*B*-O2*A*	88·6	O1*A*-*M*1*A*-O2*B*	90·3
O1*B*-*M*1*B*-O1*B*	86·6	O1*B*-*M*1*A*-O2*B*	94·7
O1*B*-*M*1*B*-O2*A*	89·3	O1*B*-*M*1*A*-O2*B*	97·2
O2*A*-*M*1*B*-O2*A*	95·5	O2*B*-*M*1*A*-O2*B*	98·8
Octahedral volume (Å^3)*	7·87 (1)	Octahedral volume (Å^3)	11·76 (2)
Quadratic elongation	1·004 (3)	Quadratic elongation	1·035 (2)
Angle variance	13·5	Angle variance	106·6

* See Table 3.

Table 14. *Refinement of the structure of wadeite-type* $K_2{}^{[VI]}Si^{[IV]}Si_3O_9$, *from Swanson & Prewitt* (1983), $R = 0{\cdot}020$

Hexagonal, $P6_3/m$ (C_{6h}^2), $Z = 2$, $a = 6{\cdot}6124\ (9)$, $c = 9{\cdot}5102\ (8)$ Å, $V = 360{\cdot}11\ (7)$ Å^3. Distances are given in Å and angles in °.

	Site	Symmetry	x	y	z
K	4(*f*)	3	$\frac{1}{3}$	$\frac{2}{3}$	0·05778 (5)
$^{[VI]}$Si	2(*b*)	$\bar{3}$	0	0	0
$^{[IV]}$Si	6(*h*)	*m*	0·36532 (7)	0·23343 (7)	$\frac{1}{4}$
O1	6(*h*)	*m*	0·49150 (18)	0·07339 (19)	$\frac{1}{4}$
O2	12(*i*)	1	0·23203 (13)	0·20907 (13)	0·10611 (8)

Si-O2 [6]	1·7783 (1)	Octahedral volume (Å^3)*	7·495 (4)
		Quadratic elongation	1·0003 (2)
O2-Si-O2 [6]	90·973 (9)	Angle variance	1·03
O2-Si-O2 [6]	89·027 (9)		

* See Table 3.

the way for Kinomura *et al.* (1975), who observed the high-pressure $^{[VI]}$Si analog, $K_2Si_4O_9$. Their polycrystalline sample was produced at 9 GPa and 1473 K.

In the silica-rich isomorph, $K_2Si_4O_9$, silicon occurs in all network-forming positions, in both four and six coordination. Each bridging O1 atom is coordinated to two $^{[VI]}$Si and two K, while O2 atoms are linked to one $^{[VI]}$Si, one $^{[IV]}$Si and two K.

Swanson & Prewitt (1983) synthesized single crystals of $K_2Si_4O_9$ in a piston-cylinder apparatus at 2·4 GPa and 1173 K. Their structure refinement (Fig. 11; Table 14) confirmed the wadeite structure type and provided details of the extremely regular silicon octahedral environment.

The anhydrous phase B ($Mg_{14}{}^{[VI]}Si^{[IV]}Si_4O_{24}$) *structure.* Studies by Ringwood & Major (1967*b*) on hydrous magnesium silicates at high pressure revealed a complex material, designated phase *B*. This structure, although frequently observed in subsequent studies of magnesium silicates, remained unidentified until Finger *et al.* (1989) obtained single crystals of a closely related anhydrous magnesium silicate, designated anhydrous phase *B*. The crystals of anhydrous phase *B*, identified as $Mg_{14}Si_5O_{24}$, facilitated the solution of both unknown structures.

Anhydrous phase *B* crystals were produced at the Mineral Physics Institute, State University of New York, Stony Brook, at 16·5 GPa and 2653 K. Routine solution by direct methods resulted in a structure that was subsequently found to be isostructural with $Mg_{14}Ge_5O_{24}$ (Von Dreele, Bless, Kostiner & Hughes, 1970). The orthorhombic (*Pmcb*) structure, based on close packing of O atoms, contains a six-layer (b = 14·2 Å) stacking sequence. Layers of the first type contain Mg and Si in octahedral coordination, while the second type of layer contains magnesium octahedra and silicon tetrahedra in an olivine arrangement (Fig. 12, Table 15). Layers are stacked 2-1-2-2-1-2. One surprising consequence of this sequence is that each silicon octahedron shares all twelve edges with adjacent magnesium octahedra.

Table 15. *Refinement of the structure of* $Mg_{14}Si_5O_{24}$ (*anhydrous phase B*), *from Finger & Prewitt* (1990), $R = 0{\cdot}040$

Orthorhombic, *Pmcb* (D_{2h}^9), $Z = 2$, $a = 5{\cdot}868\ (1)$, $b = 14{\cdot}178\ (1)$, $c = 10{\cdot}048\ (1)$ Å, $V = 835{\cdot}9$ Å^3. Distances are given in Å and angles in °.

	Site	Symmetry	x	y	z
Si1	2(*a*)	2/*m*	0	0	0
Si2	4(*h*)	*m*	$\frac{1}{2}$	0·31141 (5)	0·17445 (7)
Si3	4(*g*)	*m*	0	0·37524 (5)	0·99754 (8)
Mg1	2(*d*)	2/*m*	$\frac{1}{2}$	0	$\frac{1}{2}$
Mg2	4(*h*)	*m*	$\frac{1}{2}$	0·17460 (6)	0·35469 (9)
Mg3	2(*b*)	2/*m*	$\frac{1}{2}$	0	0
Mg4	8(*i*)	1	0·24050 (9)	0·00241 (4)	0·25354 (6)
Mg5	4(*g*)	*m*	0	0·17612 (6)	0·82058 (9)
Mg6	8(*i*)	1	0·24396 (10)	0·16958 (4)	0·08108 (6)
O1	4(*g*)	*m*	0	0·91394 (13)	0·34705 (18)
O2	4(*g*)	*m*	0	0·57564 (12)	0·35375 (19)
O3	4(*g*)	*m*	0	0·24165 (12)	0·49605 (19)
O4	4(*h*)	*m*	$\frac{1}{2}$	0·08599 (13)	0·17186 (18)
O5	4(*h*)	*m*	$\frac{1}{2}$	0·42488 (12)	0·16958 (19)
O6	4(*h*)	*m*	$\frac{1}{2}$	0·76001 (13)	0·47153 (16)
O7	8(*i*)	1	0·2342 (2)	0·08741 (8)	0·42136 (11)
O8	8(*i*)	1	0·2147 (2)	0·42653 (8)	0·42534 (12)
O9	8(*i*)	1	0·2824 (2)	0·76221 (8)	0·25276 (12)

Si1-O2 [2]	1·818 (2)	O8-Si1-O8 [2]	88·9
Si1-O8 [4]	1·797 (1)	O8-Si1-O8 [2]	91·1
Mean Si1-O	1·804	Octahedral volume (Å^3)*	7·846 (8)
O2-Si1-O8 [4]	89·7	Quadratic elongation	1·0002 (3)
O2-Si1-O8 [4]	90·3	Angle variance	0·5

* See Table 3.

Details of the structure are provided by Finger, Hazen & Prewitt (1991).

The phase B [$Mg_{12}{}^{[VI]}Si^{[IV]}Si_3O_{19}(OH)_2$] *structure.* The phase *B* structure was solved by Finger *et al.* (1989), who recognized its close similarity to anhydrous phase *B* and identified its composition as $Mg_{12}Si_4O_{19}(OH)_2$. Single crystals, synthesized at 12 GPa and 1473 K, display similar cell parameters (both structures have b and c axes of about 14·2 and 10·0 Å, respectively). The six-layer arrangement is similar in hydrous and anhydrous phase *B*, but the presence of OH causes periodic offsets in the layers and thus reduction to monoclinic ($P2_1/c$) symmetry. Details of the structure are given by Finger *et al.* (1991) (see Fig. 13 and Table 16).

Room-pressure framework structures with $^{[VI]}$Si

The SiP_2O_7-I *structure.* Three polymorphs of silicon diphosphate, SiP_2O_7, have been synthesized at low pressure. In each phase pairs of phosphate tetrahedra join to form P_2O_7 groups that are cross linked by SiO_6 octahedra. All O atoms in these framework structures are two-coordinated, either to two P or to one P and one Si.

Cubic (*Pa*3) SiP_2O_7-I is topologically identical to ZrP_2O_7 (Tillmanns, Gebert & Baur, 1973) (Table 17), but it adopts a superstructure of lower symmetry. In

Table 16. *Refinement of the structure of* $Mg_{12}Si_4O_{19}(OH)_2$ *(phase B), from Finger & Prewitt (1990),* $R = 0{\cdot}080$

Monoclinic, $P2_1/c$ (C_{2h}^5), $Z = 4$, $a = 10{\cdot}588\ (2)$, $b = 14{\cdot}097\ (1)$, $c = 10{\cdot}073\ (1)$ Å, $\beta = 104{\cdot}10\ (3)°$, $V = 1458{\cdot}4\ (3)$ Å^3. Distances are given in Å and angles in °.

	Site	Symmetry	x	y	z
Si1	4(*e*)	1	0·79007 (9)	0·00099 (8)	0·07415 (10)
Si2	4(*e*)	1	0·49753 (9)	0·18964 (7)	0·67358 (10)
Si3	4(*e*)	1	0·21336 (10)	0·12550 (7)	0·42675 (10)
Si4	4(*e*)	1	0·78120 (10)	0·12333 (7)	0·57300 (10)
Mg1	2(*d*)	$\bar{1}$	$\frac{1}{2}$	0	$\frac{1}{2}$
Mg2	4(*e*)	1	0·49776 (11)	0·17451 (9)	0·35639 (12)
Mg3	2(*b*)	$\bar{1}$	$\frac{1}{2}$	0	0
Mg4	4(*e*)	1	0·65272 (11)	0·00249 (12)	0·29314 (10)
Mg5	4(*e*)	1	0·07515 (11)	0·00035 (10)	0·15240 (11)
Mg6	4(*e*)	1	0·06509 (11)	0·00035 (10)	0·63472 (12)
Mg7	4(*e*)	1	0·35160 (11)	0·00277 (10)	0·21545 (12)
Mg8	4(*e*)	1	0·64927 (11)	0·16994 (9)	0·12361 (12)
Mg9	4(*e*)	1	0·07005 (11)	0·17303 (9)	0·96971 (12)
Mg10	4(*e*)	1	0·21857 (11)	0·17720 (9)	0·75197 (11)
Mg11	4(*e*)	1	0·77446 (11)	0·17593 (9)	0·89486 (12)
Mg12	4(*e*)	1	0·35095 (11)	0·16857 (9)	0·04510 (12)
Mg13	4(*e*)	1	0·93431 (11)	0·17750 (9)	0·19882 (12)
O1	4(*e*)	1	0·4984 (2)	0·0752 (2)	0·6696 (2)
O2	4(*e*)	1	0·6474 (2)	0·0869 (2)	0·4613 (2)
O3	4(*e*)	1	0·7832 (2)	0·2400 (2)	0·5726 (2)
O4	4(*e*)	1	0·7830 (2)	0·0858 (2)	0·7289 (2)
O5	4(*e*)	1	0·2152 (2)	0·2425 (2)	0·4249 (2)
O6	4(*e*)	1	0·3472 (2)	0·0875 (2)	0·3842 (2)
O7	4(*e*)	1	0·2104 (2)	0·0871 (2)	0·5816 (2)
O8	4(*e*)	1	0·0806 (2)	0·0881 (2)	0·3171 (2)
O9	4(*e*)	1	0·4989 (2)	0·2413 (2)	0·5293 (2)
O10	4(*e*)	1	0·6203 (2)	0·2386 (2)	0·7795 (2)
O11	4(*e*)	1	0·5002 (2)	0·0851 (2)	0·1721 (2)
O12	4(*e*)	1	0·6667 (2)	0·0744 (2)	0·9698 (2)
O13	4(*e*)	1	0·7928 (2)	0·0757 (2)	0·2192 (2)
O14	4(*e*)	1	0·0863 (2)	0·0714 (2)	0·8220 (2)
O15	4(*e*)	1	0·9182 (2)	0·0796 (2)	0·0279 (2)
O16	4(*e*)	1	0·3331 (2)	0·0734 (2)	0·8838 (2)
O17	4(*e*)	1	0·2088 (2)	0·0729 (2)	0·0711 (2)
O18	4(*e*)	1	0·3748 (2)	0·2392 (2)	0·7155 (2)
O19	4(*e*)	1	0·9116 (2)	0·0852 (2)	0·5285 (2)
O20	4(*e*)	1	0·0675 (2)	0·2477 (2)	0·6369 (2)
O21	4(*e*)	1	0·9218 (2)	0·2481 (2)	0·3639 (2)
H1	4(*e*)	1	0·025 (5)	0·193 (4)	0·600 (5)
H2	4(*e*)	1	0·918 (5)	0·204 (4)	0·416 (5)

Si1-O12	1·795 (3)	O12-Si-O13	90·3 (1)
Si1-O13	1·797 (3)	O12-Si-O14	179·6 (1)
Si1-O14	1·787 (3)	O12-Si-O15	89·0 (1)
Si1-O15	1·897 (3)	O12-Si-O16	90·4 (1)
Si1-O16	1·804 (3)	O12-Si-O17	90·2 (1)
Si1-O17	1·800 (3)	O13-Si-O14	89·6 (1)
		O13-Si-O15	89·2 (1)
Mean Si1-O	1·813	O13-Si-O16	91·1 (1)
Octahedral volume (Å^3)*	7·919 (12)	O13-Si-O17	178·6 (1)
Quadratic elongation	1·0008 (19)	O14-Si-O15	90·6 (1)
Angle variance	0·4	O14-Si-O16	90·0 (1)
		O14-Si-O17	89·9 (11)
		O15-Si-O16	179·3 (1)
		O15-Si-O17	89·5 (1)
		O16-Si-O17	90·2 (1)

* See Table 3.

Table 17. *Refinement of the* SiP_2O_7-I *structure, from Tillmanns et al.* (1973), $R = 0{\cdot}061$

Cubic, $Pa\bar{3}$ (T_h^6), $Z = 4$, $a = 7{\cdot}473\ (1)$ Å, $V = 417{\cdot}34\ (5)$ Å^3. Distances are given in Å and angles in °.

	Site	Symmetry	x	y	z
Si	4(*a*)	$\bar{3}$	0	0	0
P	8(*c*)	3	0·3833 (5)	x	x
O1	4(*b*)	$\bar{3}$	$\frac{1}{2}$	$\frac{1}{2}$	$\frac{1}{2}$
O2	24(*d*)	1	0·441 (2)	0·202 (2)	0·408 (2)

Substructure Si octahedra

Si-O1 [6]	1·716	Octahedral volume (Å^3)*	6·74 (7)
		Quadratic elongation	1·001 (3)
O2-Si-O2 [6]	88·7	Angle variance	2·0
O2-Si-O2 [6]	91·3		

Proposed superstructure Si octahedra

Mean Si-O	Approximate volume (Å^3)
1·730	6·9
1·750	7·1
1·750	7·1
1·755	7·2
1·755	7·2
1·758	7·2

* See Table 3.

the $Pa\bar{3}$ substructure Si-O bonds would be unusually short - only 1·716 Å - yielding a near regular octahedron with by far the smallest volume [6·74 (7) Å^3] of any known [VI]Si site. This aristotype structure is also unusual in that P-O-P bonds lie along a threefold axis, so the P-O-P angle is constrained to be 180°.

To compensate for these unfavorable features, the SiP_2O_7-I structure undergoes framework tilting to a lower-symmetry form. Tillmanns *et al.* (1973) proposed a tilted structure with six symmetrically independent octahedra. The mean Si-O distances of these octahedra, ranging from 1·730 to 1·758 Å, are still unusually short but are at least closer to those of other framework [VI]Si compounds.

The SiP_2O_7-III *structure.* The monoclinic ($P2_1/c$) SiP_2O_7-III structure features sharply bent P_2O_7 dimers, with 139·2° P-O-P angles (Bissert & Liebau, 1970). All ten symmetrically distinct atoms in the structure are in the general position, but the silicon octahedron is close to regular (Table 18).

The SiP_2O_7-IV *structure.* Liebau & Hesse (1971) solved the SiP_2O_7-IV structure and an improved refinement was published by Hesse (1979) (Table 19). The monoclinic ($P2_1/n$) arrangement is topologically similar to SiP_2O_7-III. The P-O-P angle is 133° and the Si octahedron is close to regular.

The $^{[VI]}Si_3{}^{[IV]}Si_2P_6O_{25}$ *structure.* The crystal structure of $Si_5P_6O_{25}$ was reported by Mayer (1974), following the solution of the isostructural compound $Ge_5P_6O_{25}$ (Mayer & Vollenkle, 1972). Isolated Si octahedra and pairs of Si tetrahedra (Si_2O_7) are cross linked by P tetrahedra to form a three-dimensional framework. Structural details appear in Table 20. Subsequent synthesis of $^{[VI]}Ge_3{}^{[IV]}Si_2P_6O_{25}$ by Leclaire & Raveau (1988) emphasizes the close relationship between structures containing octahedral Ge and Si.

The $(NH_4)_2SiP_3O_{13}$ *structure.* Durif, Averbuch-Pouchot & Guitel (1976) solved the complex triclinic ($P\bar{1}$) structure of $(NH_4)_2SiP_3O_{13}$, which contains four-tetrahedra P_4O_{13} chain-like groups linked by Si

Table 18. *Refinement of the* SiP_2O_7-III *structure, from Bissert & Liebau* (1970), $R = 0{\cdot}070$

Monoclinic, $P2_1/c$ (C_{2h}^5), $Z = 4$, $a = 4{\cdot}73$, $b = 6{\cdot}33$, $c = 14{\cdot}71$ Å, $\beta = 90{\cdot}1°$, $V = 440{\cdot}4$ Å^3. Distances are given in Å and angles in °.

	x	y	z
Si*	0·2495 (4)	0·0825 (3)	0·1353 (1)
P1	0·7457 (4)	0·8080 (3)	0·0725 (1)
P2	0·7381 (4)	0·3937 (3)	0·1684 (1)
O1	0·7110 (13)	0·5622 (10)	0·0881 (4)
O2	0·6607 (12)	0·8314 (1)	−0·0248 (4)
O3	0·5449 (12)	0·9171 (9)	0·1376 (4)
O4	0·0498 (12)	0·8643 (10)	0·0916 (4)
O5	0·9507 (13)	0·2404 (10)	0·1311 (4)
O6	0·4515 (12)	0·2951 (10)	0·1794 (4)
O7	0·8387 (13)	0·5084 (10)	0·2525 (4)

Si-O2	1·766	O3-Si-O4	88·1
Si-O3	1·746	O3-Si-O5	178·2
Si-O4	1·793	O3-Si-O6	91·0
Si-O5	1·732	O3-Si-O7	90·6
Si-O6	1·774	O4-Si-O5	90·1
Si-O7	1·765	O4-Si-O6	173·4
Mean Si-O	1·763	O4-Si-O7	90·4
		O5-Si-O6	90·8
O2-Si-O3	90·7	O5-Si-O7	89·7
O2-Si-O4	92·0	O6-Si-O7	89·2
O2-Si-O5	89·1		
O2-Si-O6	88·5	Octahedral volume (Å^3)†	7·30 (3)
O2-Si-O7	177·4	Quadratic elongation	1·001 (2)
		Angle variance	1·3

* All atoms in general position 4(*e*).
† See Table 3.

Table 19. *Refinement of the* SiP_2O_7-IV *structure, from Hesse* (1979), $R = 0{\cdot}050$

Monoclinic, $P2_1/n$ (C_{2h}^5), $Z = 4$, $a = 4{\cdot}713$ (1), $b = 11{\cdot}987$ (2), $c = 7{\cdot}628$ (2) Å, $\beta = 91{\cdot}20$ (2)°, $V = 430{\cdot}8$ (1) Å^3. Distances are given in Å and angles in °.

	x	y	z
Si*	0·2195 (4)	0·8505 (2)	0·3474 (3)
P1	0·7991 (4)	0·5182 (2)	0·1962 (2)
P2	0·7203 (4)	0·6970 (2)	0·4483 (3)
O1	0·7073 (10)	0·5725 (4)	0·3743 (6)
O2	0·0805 (10)	0·4645 (4)	0·2364 (6)
O3	0·5788 (10)	0·4350 (4)	0·1412 (6)
O4	0·8249 (10)	0·6109 (4)	0·0651 (6)
O5	0·6224 (9)	0·6873 (4)	0·6315 (6)
O6	0·0215 (10)	0·7364 (4)	0·4303 (6)
O7	0·5153 (9)	0·7624 (4)	0·3379 (6)

Si-O2	1·786 (5)	O3-Si-O4	90·7 (3)
Si-O3	1·736 (5)	O3-Si-O5	90·1 (3)
Si-O4	1·784 (5)	O3-Si-O6	90·0 (3)
Si-O5	1·759 (5)	O3-Si-O7	178·5 (3)
Si-O6	1·779 (5)	O4-Si-O5	178·9 (2)
Si-O7	1·752 (5)	O4-Si-O6	90·4 (3)
Mean Si-O	1·766	O4-Si-O7	89·3 (3)
		O5-Si-O6	90·4 (3)
O2-Si-O3	90·3 (3)	O5-Si-O7	89·9 (3)
O2-Si-O4	89·8 (3)	O6-Si-O7	88·6 (3)
O2-Si-O5	89·5 (3)		
O2-Si-O6	179·7 (3)	Octahedral volume (Å^3)†	7·34 (2)
O3-Si-O7	91·1 (3)	Quadratic elongation	1·000 (5)
		Angle variance	0·5

* All atoms in general position 4(*e*).
† See Table 3.

octahedra (Table 21). Each Si octahedron contacts four phosphate chains to create a three-dimensional framework. The NH_4 groups lie between adjacent P chains.

Table 20. *Refinement of the* $Si_5P_6O_{25}$ *structure from Mayer* (1974), $R = 0{\cdot}060$

Rhombohedral, $R\bar{3}$ (C_{3i}^2), $Z = 3$, $a = 7{\cdot}86$ (9), $c = 24{\cdot}13$ (8) Å, $V = 1294{\cdot}5$ (10) Å^3. Distances are given in Å and angles in °.

	Site	Symmetry	x	y	z
Si1	3(*a*)	$\bar{3}$	0	0	0
Si2	6(*c*)	3	0	0	0·1797 (1)
Si3	6(*c*)	3	0	0	0·4340 (1)
P	18(*f*)	1	0·2863 (3)	0·2675 (3)	0·0924 (1)
O1	3(*b*)	$\bar{3}$	0	0	$\frac{1}{2}$
O2	18(*f*)	1	0·1309 (7)	0·2136 (8)	0·1372 (2)
O3	18(*f*)	1	0·2095 (8)	0·1459 (7)	0·0403 (2)
O4	18(*f*)	1	0·3549 (8)	0·4871 (8)	0·0769 (2)
O5	18(*f*)	1	0·4602 (8)	0·2530 (8)	0·1116 (2)

Si1-O3 [6]	1·758	Octahedral volume (Å^3)*	7·22 (3)
		Quadratic elongation	1·002 (1)
O3-Si1-O3 [6]	87·7	Angle variance	5·9
O3-Si1-O3 [6]	92·3		

* See Table 3.

Table 21. *Refinement of the* $(NH_4)_2SiP_4O_{13}$ *structure, from Durif et al.* (1976), $R = 0{\cdot}035$

Triclinic, $P\bar{1}$ (C_i^1), $Z = 2$, $a = 15{\cdot}14$ (1), $b = 7{\cdot}684$ (5), $c = 4{\cdot}861$ (5) Å, $\alpha = 97{\cdot}86$ (1), $\beta = 96{\cdot}74$ (1), $\gamma = 83{\cdot}89$ (1)°, $V = 553{\cdot}97$ Å^3. Distances are given in Å and angles in °.

	x	y	z
Si*	0·75896 (6)	0·0618 (1)	0·0439 (2)
P1	0·85025 (5)	0·2134 (1)	0·6039 (1)
P2	0·69218 (6)	0·6806 (1)	0·1797 (2)
P3	0·78874 (5)	0·6806 (1)	0·1797 (2)
P4	0·66334 (5)	0·9138 (1)	0·4800 (1)
O1	0·9367 (1)	0·2872 (3)	0·6948 (5)
O2	0·8281 (1)	0·764 (3)	0·7814 (4)
O3	0·8445 (1)	0·1365 (3)	0·2960 (4)
O4	0·7704 (2)	0·3706 (3)	0·6272 (5)
O5	0·6032 (2)	0·4221 (3)	0·6638 (5)
O6	0·7093 (1)	0·2806 (3)	0·0342 (4)
O7	0·7076 (1)	0·6003 (3)	0·9791 (4)
O8	0·8654 (2)	0·5528 (3)	0·2301 (5)
O9	0·8076 (1)	0·8417 (3)	0·0537 (4)
O10	0·7414 (1)	0·7522 (3)	0·4523 (4)
O11	0·5748 (2)	0·8509 (3)	0·3834 (5)
O12	0·6894 (1)	0·0485 (3)	0·3060 (4)
O13	0·6721 (1)	0·9846 (3)	0·7892 (4)
N1	0·4940 (2)	0·7438 (4)	0·8266 (6)
N2	0·0322 (2)	0·3140 (5)	0·2310 (6)

Si-O2	1·765	Mean Si-O	1·771
Si-O3	1·761		
Si-O6	1·772	Octahedral volume (Å^3)†	7·39 (1)
Si-O9	1·776	Quadratic elongation	1·001 (2)
Si-O12	1·765	Angle variance	4·3
Si-O13	1·788		

* All atoms in general position 2(*i*).
† See Table 3.

The thaumasite $[Ca_3Si(OH)_612H_2O(SO_4)(CO_3)]$ *structure.* Thaumasite, a hydrothermal mineral formed in near-surface (*i.e.* low pressure) veins and cavities, is the only known mineral with $Si(OH)_6$ octahedra. The hexagonal ($P6_3$) structure was described by Edge & Taylor (1971), and an improved refinement was given by Effenberger, Kirfel, Will & Zobetz (1983) (Table 22). These authors recognized that structural columns of approximate composition $^{[VIII]}Ca_3{}^{[VI]}Si(OH)_6.12H_2O$ run parallel to **c**. The SO_4

Table 22. *Refinement of the structure of thaumasite,* $Ca_3(H_2O)_{12}[Si(OH)_6](CO_3)(SO_4)$, *from Effenberger et al.* (1983), $R = 0{\cdot}027$

Hexagonal, $P6_3$ (C_6^6), $Z = 2$, $a = 11{\cdot}030\,(7)$, $c = 10{\cdot}396\,(6)$ Å, $V = 1095{\cdot}3\,(6)$ Å^3. Distances are given in Å and angles in °.

	Site	Symmetry	x	y	z
Ca*	6(*c*)	1	0·19486 (5)	0·98829 (5)	0·25133†
Si	2(*a*)	3	0	0	0·0026 (2)
C	2(*b*)	3	$\frac{1}{3}$	$\frac{2}{3}$	0·4660 (6)
S	2(*b*)	3	$\frac{1}{3}$	$\frac{2}{3}$	0·9847 (2)
O1	6(*c*)	1	0·3910 (2)	0·2282 (2)	0·2546 (4)
O2	6(*c*)	1	0·2618 (2)	0·4024 (2)	0·2521 (4)
O3	6(*c*)	1	0·0029 (3)	0·3395 (3)	0·0719 (4)
O4	6(*c*)	1	0·0242 (4)	0·3485 (3)	0·4329 (4)
O5	6(*c*)	1	0·2010 (3)	0·6229 (3)	0·4602 (3)
O6	6(*c*)	1	0·1920 (3)	0·6227 (3)	0·0337 (3)
O7	6(*c*)	1	0·1304 (3)	0·1245 (3)	0·1071 (3)
O8	6(*c*)	1	0·1308 (3)	0·1250 (3)	0·3981 (3)
O9	2(*b*)	3	$\frac{1}{3}$	$\frac{2}{3}$	0·8436 (4)

Si-O7 [3]	1·778 (3)	O7-Si-O8	93·4 (1)
Si-O8 [3]	1·781 (3)	O8-Si-O8	86·7 (1)
Mean Si-O	1·779	Octahedral volume (Å^3)‡	7·48 (2)
O7-Si-O7	86·5 (2)	Quadratic elongation	1·003 (1)
		Angle variance	12·5

* Positions of ten H atoms not listed.
† z coordinate of Ca held constant.
‡ See Table 3.

and CO_3 groups lie in between these columns. The silicon octahedron is relatively undistorted, with three longer (1·781 Å) and three shorter (1·778 Å) bonds and O-Si-O angles between 86·5 and 93·4°. The octahedral volume (7·50 Å^3) and interoctahedral angles are typical of other $^{[VI]}$Si polyhedra.

Systematics of $^{[VI]}$Si coordination

Octahedral Si-O distances, polyhedral volumes, distortion indices and interpolyhedral linkages for $^{[VI]}$Si structure types described above are summarized in Table 23. Of special interest is the variety of linkages between Si octahedra and other octahedra and tetrahedra. The four low-pressure silicon phosphates feature low-density corner-linked arrays of tetrahedra and octahedra. Dense high-pressure phases, however, commonly incorporate shared edges between octahedra. In stishovite, hollandite and pyroxene a combination of edge and corner sharing is observed, but in phase *B* and anhydrous phase *B* each Si octahedron shares all 12 edges with adjacent Mg octahedra. In pyrochlore, garnet and wadeite the Si octahedra form part of a corner-linked framework, but additional cations in eight or greater coordination share edges and faces with the octahedra. Ilmenite presents yet a different topology, with unusual face sharing between Mg and Si octahedra, as well as corner and edge sharing.

In spite of the variety of polyhedral linkages, the size and shape of SiO_6 polyhedra are similar in all these compounds. Polyhedral volumes vary by only about ±4% from an average 7·57 Å^3 value. All Si octahedra are close to regular (*i.e.* distortion indices are small) relative to the range observed for many divalent and trivalent cation octahedra. These trends are consistent with the observation of Robert Downs (personal communication) that SiO_6 groups, in all structures for which anisotropic thermal parameters have been determined, display rigid-body vibrational motion. Similar behavior is displayed by SiO_4 and AlO_4 tetrahedra in silicates (Downs, Gibbs & Boisen, 1990). Stebbins & Kanzaki (1991) used the distinctive NMR signature of these rigid groups to determine structural characteristics of a number of as yet unidentified $^{[VI]}$Si phases in the system Ca-Si-O.

Baur (1977) noted a strong correlation between oxygen coordination number and mean octahedral Si-O distance. He proposed the approximate relation:

$$(\text{Si-O})_{\text{mean}} = 1{\cdot}729 + 0{\cdot}013CN,$$

where CN is the mean coordination number of O atoms in the octahedron. This trend, although expected from bond length-bond strength systematics, leads to the situation that dense high-pressure silicates (with higher oxygen coordination) also display the longest Si-O bond distances. This trend is evident from the data in Table 23. Two-coordinated O atoms in the room-pressure framework silicon phosphates are accompanied by mean $^{[VI]}$Si-O that are relatively short, averaging just 1·73 Å, with polyhedral volumes less than 7·4 Å^3. The dense high-pressure $^{[VI]}$Si phases, on the other hand, have O atoms in three or four coordination. Mean Si-O bond lengths in these compounds average greater than 1·78 Å, while octahedral volumes average almost 7·7 Å^3.

Other possible $^{[VI]}$Si structures

The 18 structure types detailed above form an eclectic group of silicate compositions and topologies. A few systematic relations among the structures, however, can be used to predict other possible $^{[VI]}$Si phases. These criteria include:

1. Three structure types (rutile, hollandite, calcium ferrite) are formed from edge-sharing chains of silicon octahedra.

2. Most of the high-pressure silicate structures were first synthesized at room pressure as germanate isomorphs.

3. All seven high-pressure $^{[VI]}$Si structures without tetrahedral Si are isomorphs of room-pressure oxides with trivalent or tetravalent transition metals (Ti, Mn or Fe) in octahedral coordination.

4. Three high-pressure magnesium silicates (ilmenite, garnet, pyroxene) are derived from room-pressure $^{[VI]}$Al structures by the substitution $2\,^{[VI]}\text{Al} \rightarrow {}^{[VI]}(\text{Mg} + \text{Si})$.

Table 23. *Summary of octahedral sizes, distortions and linkages for* $^{[VI]}$Si

Structure	Min. Si-O (Å)	Max. Si-O (Å)	Mean Si-O (Å)	Octahedral volume (Å^3)	Quadratic elongation	Angle variance	Interpolyhedral linkages* Corners	Edges	Faces
SiO_2 stishovite	1·757	1·809	1·774	7·36	1·008	27	4 to $^{[VI]}$Si; 2 to $2^{[VI]}$Si	2 to $^{[VI]}$Si	-
$CaSiO_3$ perovskite	1·784	1·784	1·784	7·55	1	0	6 to $^{[VI]}$Si	-	-
$MgSiO_3$ perovskite	1·783	1·801	1·793	7·63	1·001	2			
$MgSiO_3$ ilmenite	1·768	1·830	1·799	7·59	1·015	53	3 to $^{[VI]}$Mg; 3 to $2^{[VI]}$Mg	3 to $^{[VI]}$Si	1 to $^{[VI]}$Mg
$KAlSi_3O_8$ hollandite†	1·71	1·97	1·81	7·62	1·02	61	3 to $^{[VI]}$Si	4 to $^{[VI]}$Si	-
Sc_2SiO_7 pyrochlore	1·761	1·761	1·761	7·26	1·002	7	6 to $^{[VI]}$Si	-	-
$In_2Si_2O_7$ pyrochlore	1·800	1·800	1·800	7·71	1·005	8		-	-
$MgSiO_3$ garnet‡	1·792	1·826	1·807	7·86	1·000	1	6 to $^{[IV]}$Si	-	-
$MnSiO_3$ garnet	1·757	1·805	1·795	7·69	1·001	3			
$NaMg_{0.5}{}^{[VI]}Si_{0.5}{}^{[IV]}Si_2O_6$ pyroxene	1·782	1·826	1·811	7·87	1·004	14	6 to $^{[IV]}$Si	2 to $^{[VI]}$Mg	-
$K_2{}^{[VI]}Si^{[IV]}Si_3O_9$ wadeite	1·797	1·818	1·804	7·85	1·000	1	6 to $^{[IV]}$Si	-	-
$Mg_{14}{}^{[VI]}Si^{[IV]}Si_4O_{24}$	1·797	1·818	1·804	7·85	1·000	1	-	12 to $^{[VI]}$Mg	-
$Mg_{12}{}^{[VI]}Si^{[IV]}Si_3O_{19}(OH)_2$	1·787	1·897	1·813	7·92	1·001	0	-	12 to $^{[VI]}$Mg	-
SiP_2O_7-III	1·732	1·793	1·863	7·30	1·001	1	6 to $^{[IV]}$P	-	-
SiP_2O_7-IV	1·736	1·786	1·766	7·34	1·000	1	6 to $^{[IV]}$P	-	-
$^{[VI]}Si_3{}^{[IV]}Si_2P_6O_{25}$	1·758	1·758	1·758	7·22	1·002	6	6 to $^{[IV]}$P	-	-
$(NH_4)_2SiP_4O_{13}$	1·761	1·788	1·771	7·39	1·001	4	6 to $^{[IV]}$P	-	-

* Linkages to octahedra and tetrahedra only.
† Site composition constrained to be $Si_{0.75}Al_{0.25}$.
‡ Site composition refined to be $Si_{0.80}Mg_{0.20}$.

5. Phase *B* and anhydrous phase *B* are closely related structures that form a homologous series of phases in the Mg-Si-O-H system.

Each of these criteria can be used to predict other potential $^{[VI]}$Si phases.

High-pressure silicates with $^{[VI]}$Si *edge-sharing chains*

The close structural relationship among rutile, hollandite and calcium ferrite - three of the seven known high-pressure structures with all silicon in octahedral coordination - suggests a number of other likely structure types. All of these structures consist of edge-sharing octahedral chains that are linked to adjacent strips by corner sharing, as systematized by Wadsley (1964), Bursill & Hyde (1972) and Bursill (1979). Rutile has single chains, leading to 1×1 square channels, while hollandite and calcium ferrite have double chains, yielding larger channels. Many similar octahedral chain structures, such as ramsdellite (1×2) and psilomelane (2×3), are also known (Fig. 14) and each of these could provide a topology suitable for silicon in six coordination (Table 24).

Bursill (1979) explored a wide variety of hypothetical MX_2 structures created by juxtaposition of single-, double- and triple-width octahedral chains. Both ordered and disordered phases with mixtures of rutile, ramsdellite, hollandite and psilomelane channels were examined. A surprising feature of these structures is that all could be constructed from the simple stoichiometry, SiO_2. In fact, most of the compounds in this group of structures display coupled substitution of a channel-filling alkali or alkaline-earth cation plus Al for the octahedral cation. Only

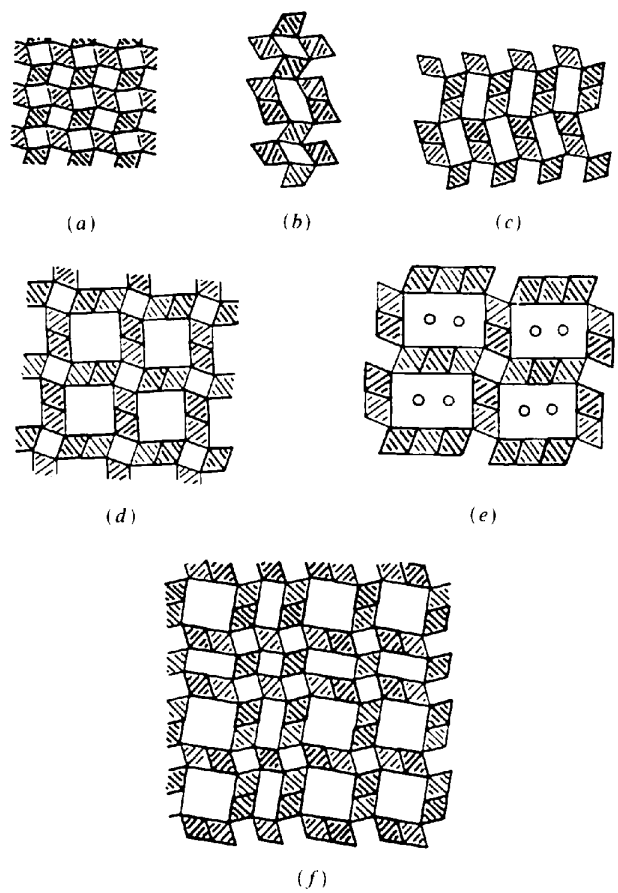

Fig. 14. Relationships among the rutile (*a*), $IrSe_2$ (*b*), ramsdellite (*c*), hollandite (*d*), psilomelane (*e*) and a hypothetical composite structure (*f*), after Bursill (1979).

Table 24. *Predicted and observed high-pressure* $^{[VI]}$Si *compounds, based on edge-sharing chains of octahedra*

Composition*	Structure type	Chain widths	Channel shape and size
SiO_2†	Rutile	1	Square 1×1
$KAlSi_3O_8$† $BaAl_2Si_2O_8$†	Hollandite	2	Square 2×2 and 1×1
$KAlSi_5O_{12}$ $BaAl_2Si_4O_{12}$	Todorokite‡	3	Square 3×3 and 1×1
SiO_2 $(MgSi)O_2(OH)_2$	Ramsdellite Diaspore	2	Rectangular 1×2
$KAlSi_2O_6$ $BaAl_2SiO_6$	$IrSe_2$	1 and 2	Rectangular 1×2 and 1×1
$KAlSi_3O_8$ $BaAl_2Si_2O_8$	?	1 and 3	Rectangular 1×3 and 1×1
$KAlSi_4O_{10}$ $BaAl_2Si_3O_{10}$	Romanechite‡	2 and 3	Rectangular 2×3 and 1×1
$NaAlSiO_4$†	Calcium ferrite	2	Triangular 2×2×(1+1)

* All of these octahedral chain structures could have composition SiO_2. Al substitution for Si is coupled with introduction of alkali or alkaline earth in channels.

† Known $^{[VI]}$Si phase.

‡ Todorokite and romanechite are unlikely candidates for high-pressure structures owing to their large channels.

the structures of rutile (TiO_2), iridium selenide ($IrSe_2$) and ramsdellite (γ-MnO_2) are known without additional cations in the channels.

Bursill (1979) extended his discussion to a number of more-complex structures that combine the MX_2 forms described above with β-Ga_2O_3 topology, which is based on the same type of double edge-shared chains as found in hollandite. A range of gallium titanates, such as Ga_4TiO_8, $Ga_4Ti_7O_{20}$ and $Ga_4Ti_{21}O_{48}$ (all members of the homologous series $Ga_4Ti_{m-4}O_{2m-2}$ that couple rutile and γ-Ga_2O_3 units) are illustrated, as are ternary Ba–Ga–Ti oxides that unite components of rutile, hollandite and γ-Ga_2O_3. All of these phases could accommodate $^{[VI]}$Si at high pressure.

Silicates based on substitution of $^{[VI]}$Si *for* $^{[VI]}$Ge

Nine of the twelve known $^{[VI]}$Si high-pressure structure types were first synthesized as germanates at lower pressures. We have conducted a systematic search of the Inorganic Crystal Structure Database (ICSD, FIZ, Karlsruhe, Germany) for germanates with $^{[VI]}$Ge in systems containing the additional cations Na, K, Mg, Fe, Ca, Al, Ti, Si and P. More than two dozen structure types, only nine of which have known silicate analogs, were identified (Table 25).

In predicting high-pressure silicate isomorphs of these known room-pressure germanates, it is important to take into account the relative compressibilities of the different cation polyhedra. Large monovalent and divalent cations, such as Na, K and Ca, form polyhedra that are much more compressible than tetravalent Ge or Si. Since the stability of many structures depends critically on the cation radius ratio (Pauling, 1960), it may be appropriate to substitute a smaller divalent cation when attempting to synthesize high-pressure forms. Thus, a high-pressure isomorph of $CaGe_2O_5$ might be $MgSi_2O_5$ while $CaSi_2O_5$ might be unstable.

$^{[VI]}$Si *silicate isomorphs of transition-metal oxides*

All known high-pressure silicates with all silicon as $^{[VI]}$Si adopt the structures of room-pressure oxides with Ti, Mn or Fe. Structures of other binary oxides with octahedral titanium, manganese or iron thus represent possible topologies for mantle minerals. A complete survey of the dozens of transition-metal oxide structures is beyond the scope of this review, but several promising structure types are listed in Table 26.

Numerous other octahedral transition-metal structures could be listed. For example, there are many complex Ti, Mn and Fe borates (*e.g.* Moore & Araki, 1974), based on frameworks of BO_3 triangles and columns and sheets of transition-metal octahedra. The K_2NiF_4 structure, adopted by Ca_2SiO_4 at high pressure, is just one of a wide variety of layered perovskite-related phases (Subramanian, Gopalakrishnan & Sleight, 1988; Hazen, 1990). A perplexing array of natural and synthetic tantalates, niobates and uranium compounds incorporate Ti, Mn, Fe and other transition-metal octahedra with larger irregular cation polyhedra. As the search for $^{[VI]}$Si compounds extends beyond common rock-forming elements, new $^{[VI]}$Si structures will undoubtedly be found among isomorphs of these known phases.

Silicates based on substitution of $^{[VI]}$(Si + Mg) *for* 2Al

High-pressure ilmenite, garnet and pyroxene forms of magnesium-bearing silicates are all related to room-pressure phases by the substitution of octahedral Mg and Si for a pair of aluminium cations. Similar substitutions might occur in several other common rock-forming minerals at high pressures (Table 27). Note that this substitution scheme will not work for many common aluminium-bearing minerals with mixed four- and six-coordinated aluminium. The substitution in muscovite, $K^{[VI]}Al_2{}^{[IV]}(AlSi_3)O_{10}(OH)_2$, for example, would yield the magnesian mica celadonite, $K^{[VI]}(MgAl)$-$^{[IV]}Si_4O_{10}(OH)_2$, in which all Si is tetrahedrally coordinated. Octahedral Al, thus, must constitute more than two thirds of all aluminium to produce an $^{[VI]}$Si phase by the substitution $2Al \rightarrow (Mg + Si)$.

Systematics of phase B and other high-pressure hydrous magnesium silicates

Finger & Prewitt (1990) documented the close structural relations among a number of hydrous and

Table 25. *Predicted and observed high-pressure* $^{[VI]}$Si *compounds based on the substitution* $^{[VI]}$Ge→$^{[VI]}$Si

Known $^{[VI]}$Ge compound	Structure	Analogous $^{[VI]}$Si compound	$^{[VI]}$Ge reference
GeO_2	Rutile	SiO_2*	Smyth & Bish (1988)
$MgGeO_3$	Ilmenite	$MgSiO_3$*	Ringwood & Seabrook (1962)
$MgGeO_3$	Garnet	$MgSiO_3$*	Ringwood & Major (1967*a*)
$Mg_{14}Ge_5O_{24}$	Anhydrous *B*	$Mg_{14}Si_5O_{24}$*	Von Dreele *et al.* (1970)
$Mg_{28}Ge_{7.5}O_{32}F_{10}$	-	$Mg_{28}Si_7O_{32}F_{10}$	Bless, Von Dreele, Kostiner & Hughes (1972)
$(Mg, Ni)_{10}Ge_3O_{16}$	Aerugite	$Mg_{10}Si_3O_{16}$	Fleet & Barbier (1989)
$Fe_4Ge_2O_9$	-	$Fe_4Si_2O_9$	Modaresi, Gerardin, Malaman & Gleitzer (1984)
$Fe_8Ge_3O_{18}$	-	$Fe_8Si_3O_{18}$	Agafonov, Kahn, Michel & Perez-y-Jorba (1986)
$FeGe(OH)_6$	Stottite	$MgSi(OH)_6$	Ross, Bernstein & Waychunas (1988)
$CaGeO_3$	Perovskite	$CaSiO_3$*	Marezio *et al.* (1966)
Ca_2GeO_4	K_2NiF_4	Ca_2SiO_4*	Reid & Ringwood (1970)
$CaGe_2O_5$	Sphene	$CaSi_2O_5$	Nevsky, Ilyukhin & Belov (1979)
$Ca_2Ge_7O_{16}$	-	$Ca_2Si_7O_{16}$	Nevsky, Ilyukhin, Ivanova & Belov (1979)
$Ca_4Ge_3O_{10}(H_2O)$	-	$Ca_4Si_3O_{10}(H_2O)$	Nevsky, Ilyukhin, Ivanova & Belov (1978)
$BaGe_3SiO_9$	Benitoite	$BaSi_4O_9$	Goreaud, Choisnet, Deschanvres & Raveau (1973)
$BaGe_{2.5}Si_{1.5}O_9$			
$K_2Ge_4O_9$		$K_2Si_4O_9$*	Voellenkle & Wittmann (1971)
$K_2GeSi_3O_9$	Wadeite		Reid *et al.* (1967)
$(LiNa)Ge_4O_9$		$(LiNa)Si_4O_9$	Voellenkle *et al.* (1969)
$NaAlGeO_4$	Calcium ferrite	$NaAlSiO_4$*	Ringwood & Major (1967*a*)
$Na_4SrGe_6O_{15}$	-	$Na_4SrSi_6O_{15}$	Nadezhina, Pobedimskaya & Belov (1974)
$K_2Ge(IO_3)_6$	-	$K_2Si(IO_3)_6$	Schellhaas, Hartl & Frydrych (1972)
$KH_3Ge_7O_{16}(H_2O)_3$	Related cubic (a = 7·7 Å) phases	$(Na, K, H)_4Ge_7O_{16}(H_2O)_n$	Stura, Belokoneva, Simonov & Belov (1978)
$(Na, K)_3HGe_7O_{16}(H_2O)_4$			Nowotny & Wittmann (1954)
$K_2BaGe_8O_{18}$	-	$K_2BaSi_8O_{18}$	Baumgartner & Voellenkle (1978)
$CaCu_3Ge_4O_{12}$	-	$CaCu_3Si_4O_{12}$	Ozaki, Ghedira, Chenavas, Joubert & Marezio (1977)
$Ca_3Ga_2Ge_4O_{14}$	Gehlenite-related phases	$Ca_3Ga_2Si_4O_{14}$	Belokoneva, Simonov, Batushin, Mill & Belov (1980)
$Ba_3Fe_2Ge_4O_{14}$		$Ba_3Fe_2Si_4O_{14}$	
$Pb_3Al_{10}GeO_{20}$	-	$Pb_3Al_{10}SiO_{20}$	Vinek, Voellenkle & Nowotny (1970)
$Al_{15}Ge(Nd, Pb)_{0.2}O_{9.7}$	Mullite	$Al_{15}Si(Nd, Pb)_{0.2}O_{9.7}$	Saalfeld & Klaska (1985)
$Ge_5P_6O_{25}$	-	$Si_5P_6O_{25}$*	Mayer & Voellenkle (1972)
$Ge_3Si_2P_6O_{25}$			Leclaire & Raveau (1988)

* Known $^{[VI]}$Si phase.

Table 26. *Predicted and observed high-pressure* $^{[VI]}$Si *isomorphs of* Ti, Mn *and* Fe *oxides*

Known oxide	Structure	Analogous $^{[VI]}$Si compound
TiO_2	Rutile	SiO_2*
$CaTiO_3$	Perovskite	$MgSiO_3$*
		$CaSiO_3$*
$FeTiO_3$	Ilmenite	$MgSiO_3$*
		$ZnSiO_3$*
$BaMn_8O_{16}$	Hollandite	$KAlSi_3O_8$*
		$BaAl_2Si_2O_8$*
$CaFe_2O_4$	-	$NaAlSiO_4$*
Ca_2TiO_4	K_2NiF_4	Ca_2SiO_4*
$CaZrTi_2O_7$	Pyrochlore	$Sc_2Si_2O_7$*
		$CaZrSi_2O_7$
$CaTiSiO_5$	Sphene	$CaSi_2O_5$
Fe_2TiO_5	Pseudobrookite	Fe_2SiO_5
$BaTiSi_3O_9$	Benitoite	$BaSi_4O_9$
$ZrTiO_4$	-	$ZrSiO_4$
Ga_4TiO_8	-	Ga_4SiO_8
$Ga_4Ti_7O_{20}$	-	$Ga_4Si_7O_8$
$Pb(Ti,Fe,Mn)_{24}O_{38}$	Senaite	$Pb(Si,Fe,Mn)_{24}O_{38}$

* Known $^{[VI]}$Si phase.

anhydrous magnesium silicates and used those systematics to propose several as yet unobserved structures, including high-pressure hydrous phases with octahedral silicon (Table 28). They recognized that several known phases, including chondrodite, humite, forsterite, phase *B* and anhydrous phase *B*, are members of a large group of homologous magnesium silicates that can be represented by the general formula

$$m[Mg_{4n+2}{}^{[IV]}Si_{2n}O_{8n}(OH)_4]Mg_{6n+4-2\mathrm{mod}(n,2)}{}^{[VI]}Si_{n+\mathrm{mod}(n,2)}O_{8n+4}$$

where mod(n,2) is the remainder when n is divided by 2. Finger & Prewitt (1990) examined cases where $n = 1, 2, 3, 4, \infty$ and $m = 1, 2, \infty$. Structures with octahedral silicon result for all cases where m is not infinity.

Of special interest is the proposed structure of superhydrous phase *B*, a compound predicted by the logical progression from $Mg_{14}Si_5O_{24}$ (anhydrous phase *B*) to $Mg_{12}Si_4O_{19}(OH)_2$ (phase *B*) to $Mg_{10}Si_3O_{14}(OH)_4$. The third phase, superhydrous phase *B*, bears a close topological relationship to the other two compounds (Fig. 15). Gasparik (1990) suggested that an as yet unanalyzed hydrous magnesium silicate synthesized at 18·6 GPa and 1873 K possesses this structure and further studies on that material are in progress.

Predicted structures that fulfil more than one criterion

Tables 24–28 predict $^{[VI]}$Si compounds based on completely different compositional and structural

Table 27. *Predicted and observed high-pressure* $^{[VI]}$Si *compounds based on the substitution* $2^{[VI]}Al \rightarrow {}^{[VI]}(Mg+Si)$

Structure type	Known $^{[VI]}$Al phase	Possible $^{[VI]}$Si phase
Corundum/ilmenite	Al_2O_3	$MgSiO_3$*
Pyroxene	$NaAlSi_2O_6$	$Na(Mg_{0.5}Si_{0.5})Si_2O_6$*
Garnet	$Mg_3Al_2Si_3O_{12}$	$Mg_3(MgSi)Si_3O_{12}$*
Pseudobrookite	Al_2TiO_5	$(MgSi)TiO_5$
Gibbsite	$Al(OH)_3$	$(MgSi)(OH)_6$
Diaspore	$AlO(OH)$	$(MgSi)O_2(OH)_2$
Kyanite	Al_2SiO_5	$(MgSi)SiO_5$
Staurolite	$Fe_4Al_{18}Si_8O_{46}(OH)_2$	$Be_4Al_{14}(Mg_2Si_2)Si_8O_{46}(OH)_2$†
Clinozoisite	$Ca_2Al_3Si_3O_{12}(OH)$	$Ca_2Al(MgSi)Si_3O_{12}(OH)$
Lawsonite	$CaAl_2Si_2O_7(OH)_2H_2O$	$Ca(MgSi)Si_2O_7(OH)_2H_2O$
Cordierite	$Mg_2Si_5Al_4O_{18}$	$Mg_2Si_5(Mg_2Si_2)O_{18}$

* Known high-pressure phase.
† In staurolite Fe^{2+} is four-coordinated a configuration unlikely in a high-pressure phase. Thus Be is substituted for Fe.

Table 28. *Predicted and observed high-pressure hydrous magnesium silicates (after Finger & Prewitt, 1990)*

m*	n*	Composition	Notes
1	1	$Mg_7{}^{[VI]}Si_1{}^{[IV]}Si_1O_{10}(OH)_2$	-
1	2	$Mg_{13}{}^{[VI]}Si_1{}^{[IV]}Si_2O_{18}(OH)_2$	-
1	3	$Mg_{17}{}^{[VI]}Si_2{}^{[IV]}Si_3O_{26}(OH)_2$	-
1	4	$Mg_{23}{}^{[VI]}Si_2{}^{[IV]}Si_4O_{34}(OH)_2$	-
1	∞	$Mg_{10}{}^{[VI]}Si_1{}^{[IV]}Si_2O_{16}$	Aerugite type
2	1	$Mg_{10}{}^{[VI]}Si_1{}^{[IV]}Si_2O_{14}(OH)_4$	Superhydrous *B*
2	2	$Mg_{18}{}^{[VI]}Si_1{}^{[IV]}Si_4O_{26}(OH)_4$	-
2	3	$Mg_{24}{}^{[VI]}Si_2{}^{[IV]}Si_6O_{38}(OH)_4$	Phase *B*
2	4	$Mg_{32}{}^{[VI]}Si_2{}^{[IV]}Si_8O_{50}(OH)_4$	-
2	∞	$Mg_{28}{}^{[VI]}Si_2{}^{[IV]}Si_8O_{48}$	Anhydrous phase *B*

* Coefficients in the general structural equation:

$$m[Mg_{4n+2}{}^{[IV]}Si_{2n}O_{8n}(OH)_4]Mg_{6n+4-2\mathrm{mod}(n,2)}{}^{[VI]}Si_{n+\mathrm{mod}(n,2)}O_{8n+4}$$

where mod(n,2) is the remainder when n is divided by 2.

criteria, yet several structures types appear more than once (Table 29). These structures thus seem particularly promising for further study.

Of special interest to earth scientists are $CaSi_2O_5$ with the titanite structure, Fe_2SiO_5 with the pseudobrookite structure and $Mg_{10}Si_3O_{16}$ with the aerugite structure. Each of these phases, or their isomorphs with other cations replacing Ca, Mg and Fe, might be represented in the earth's mantle. In fact, Stebbins & Kanzaki (1991) mention the existence of titanite-type $CaSi_2O_5$, though identification of this phase was provisional.

Also worthy of further study are the proposed hydrous phases $MgSiO_2(OH)_2$ and $MgSi(OH)_6$, which are isomorphs of diaspore and stottite, respectively. Such hydrogen-rich phases would be expected

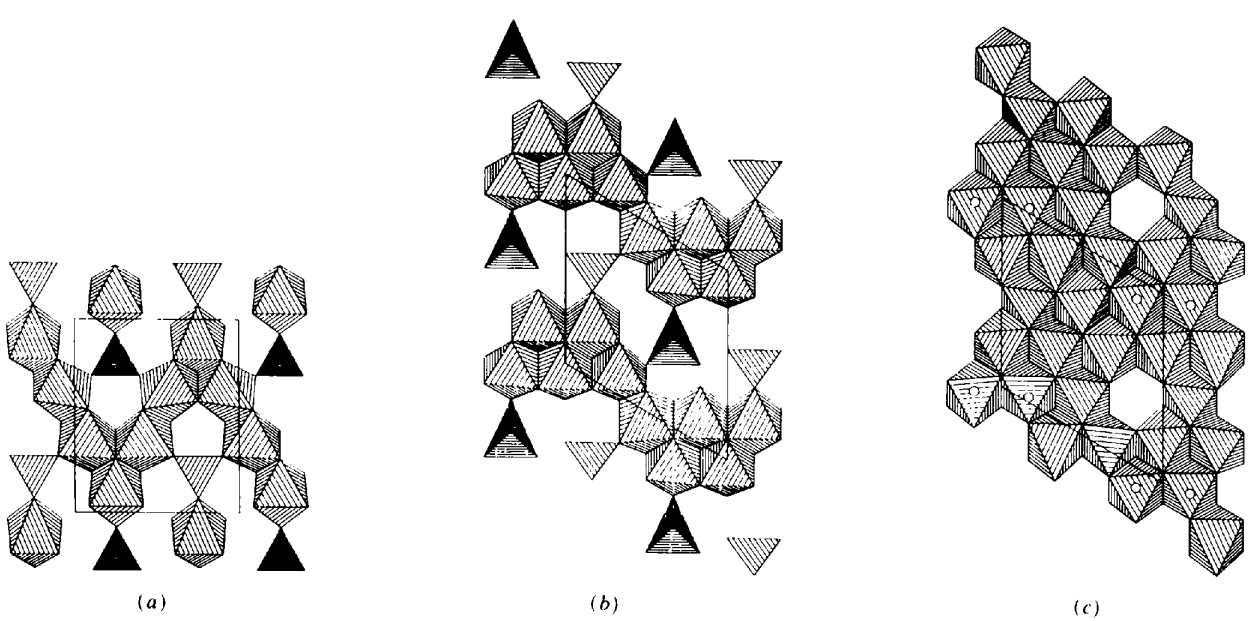

Fig. 15. Proposed structure of $Mg_{10}Si_3O_{14}(OH)_4$, superhydrous magnesium silicate structure, from Finger & Prewitt (1990). This structure includes norbergite layers (*a*), deformed as in (*b*), combined with an octahedral layer (*c*). Octahedral silicon is indicated by the small circles.

Table 29. *Predicted* [VI]Si *structures that conform to more than one criterion*

Formula	Structure	1*	2*	3*	4*	5*
$(MgSi)O_2(OH)_2$	Diaspore	×			×	
Ga_4SiO_8	—	×			×	
$Ga_4Si_7O_{20}$	—	×			×	
$Mg_{10}Si_3O_{16}$	Aerugite		×			×
$CaSi_2O_5$	Sphene		×	×		
$MgSi(OH)_6$	Stottite/gibbsite		×		×	
$BaSi_4O_9$	Benitoite		×	×		
Fe_2SiO_5	Pseudobrookite			×	×	

* Criteria for predicting [VI]Si structures: (1) Edge-sharing octahedral chains (see Table 24 and Bursill, 1979). (2) Germanate isomorphs (see Table 25). (3) Ti, Mn and Fe oxides (see Table 26). (4) Substitution of (Mg + Si) for 2Al (see Table 27). (5) System Mg-Si-O-H (see Table 28).

to occur only locally in the earth's deep interior, but their presence, integrated over the earth's volume, could represent a major repository of water.

Most common rock-forming cations, including Na, Mg, Fe, Ca, Mn, Al, Ti and Si, are small enough to fit into the tetrahedral or octahedral interstices of a close-packed oxygen net. However, the presence of many other cations, including H, B, K, Rb, Pb, rare earths and U, could disrupt the close-packed array and lead to other, as yet unrecognized, structure types. The gallium and barium silicates in Table 29 are just three of the dozens of possible new [VI]Si structures likely to be observed as high-pressure investigations extend beyond the traditional rock-forming elements. These structures are not likely to play a significant role in mantle mineralogy, but they will provide a more complete understanding of the crystal chemistry of octahedral silicon.

Concluding remarks

Is the earth's deep interior mineralogically simple? Are there only a few dominant structure types, or is there an unrecognized complexity in the crystal chemistry of octahedral silicon?

There are hundreds of different crustal silicates with [IV]Si, but only a dozen high-pressure [VI]Si structures have been produced. This disparity may reflect the relatively small number of high-pressure studies, but it also arises, at least in part, from the nature of oxygen packing. Numerous crustal silicates, from the commonest minerals quartz and feldspar to the dozens of zeolites and other framework silicates, possess open, low-density topologies with correspondingly loose packing of oxygen. There are no obvious limits to the variety of silicates based on irregular oxygen packing. For this reason, there are probably dozens of possible room-pressure silicon phosphates with open framework structures, in addition to those described above.

Volume constraints imposed by high pressure, however, favor structures with approximately close-packed O atoms. These restrictions on anion topology reduce the number of possible cation configurations as well and it is thus anticipated that the number of different structural topologies in the earth's deep interior will be much smaller than at the surface. Dense close-packed and for the most part high-symmetry structures, such as those represented by the seven known topologies with all [VI]Si (Tables 2–10), will predominate. Nevertheless, within these restrictions there exists opportunity for considerable structural diversity based on three factors – reversible phase transitions, cation positional ordering and modularity, particularly based on different close-packed layer-stacking sequences. This potential diversity is only hinted at by the known phases.

Several of the known high-pressure structure types, including perovskite, K_2NiF_4 and pyrochlore, can adopt numerous structural variants based on slight changes in lattice distortions and cation distribution. The perovskite structure, in particular, can undergo dozens of phase transitions based on octahedral tilting, cation ordering, cation displacements and anion defects (Megaw, 1973; Hazen, 1988). We must study proposed mantle phases at the appropriate conditions of pressure and temperature to document the equilibrium structural variations.

Close packing of O atoms leads to modular structures, with certain features (*e.g.* edge-sharing octahedral chains of rutile; the double chains of hollandite; the corner-sharing octahedral sheets of perovskite; the face-sharing topology of ilmenite) that can link together in many ways to form ordered superstructures of great complexity. Such complexity was recognized by Wadsley (1964) and Bursill (1979) in their descriptions of modular rutile-hollandite-β-Ga_2O_3 structures, and it is realized in the homologous series including phase *B*, anhydrous phase *B* and several other structures. Phase *B*, for example, is based on oxygen close packing, yet it has 40 independent atoms in its asymmetric unit to yield one of the most complex ternary silicates yet described. Variations on the phase-*B* structure could be based on changing the relative number and position of the two different structural layers by introducing other types of layers or by staggering layers to produce clino- and ortho-type structures as observed in other close-packed systems, for example, the biopyriboles as described by Thompson (1978) and Smith (1982). The structure could be further complicated by element ordering among the 17 different cation sites as Al, Fe, Ti, Mn and other elements enter the structure in a natural environment.

The study of octahedrally coordinated silicon is still in its infancy, yet clear trends are beginning to emerge from the scattered data on diverse structures and compositions. It is now evident that while silicate perovskite may be the predominant phase in the earth's lower mantle, a number of other dense silicate

phases will compete for elements such as K, Ba, Ca and Al. It appears that the earth's transition zone will display the varied mineralogy of mixed $^{[VI]}$Si and $^{[IV]}$Si silicates, including some of the most complex structures known in the mineral kingdom. And it is certain that a detailed understanding of the mantle must await studies of these fascinating phases at temperatures and pressures appropriate to the earth's dynamic interior.

We thank C. W. Burnham, R. J. Hemley, H. K. Mao, P. B. Moore, C. T. Prewitt and D. J. Weidner for useful discussions and constructive reviews of the manuscript. This work was supported by NSF grant EAR-8916709 for crystallographic studies of mantle minerals.

References

AGAFONOV, V., KAHN, A., MICHEL, D. & PEREZ-Y-JORBA, M. (1986). *J. Solid State Chem.* **62**, 397-401.

AKIMOTO, S. & SYONO, Y. (1972). *Am. Mineral.* **57**, 76-84.

ANDERSON, O. L. (1976). *Geophys. Res. Lett.* **3**, 347-349.

ANGEL, R. J., FINGER, L. W., HAZEN, R. M., KANZAKI, M., WEIDNER, D. J., LIEBERMANN, R. C. & VEBLEN, D. R. (1989). *Am. Mineral.* **74**, 509-512.

ANGEL, R. J., GASPARIK, T., ROSS, N. L., FINGER, L. W., PREWITT, C. T. & HAZEN, R. M. (1988). *Nature (London)*, **335**, 156-158.

BAUMGARTNER, O. & VOELLENKLE, H. (1978). *Monatsh. Chem.* **109**, 1145-1153.

BAUR, W. (1977). *J. Solid State Chem.* **22**, 445-446.

BAUR, W. H. & KHAN, A. A. (1971). *Acta Cryst.* B**27**, 2133-2138.

BELOKONEVA, E. L., SIMONOV, M. A., BATUSHIN, A. V., MILL, B. V. & BELOV, N. V. (1980). *Dokl. Akad. Nauk SSSR*, **255**, 1099-1104.

BIRCH, F. (1952). *J. Geophys. Res.* **57**, 227-286.

BISSERT, G. & LIEBAU, F. (1970). *Acta Cryst.* B**26**, 233-240.

BLESS, P. W., VON DREELE, R. B., KOSTINER, E. & HUGHES, R. E. (1972). *J. Solid State Chem.* **4**, 262-268.

BURSILL, L. A. (1979). *Acta Cryst.* B**35**, 530-538.

BURSILL, L. A. & HYDE, B. G. (1972). *Nature (London) Phys. Sci.* **240**, 122-124.

CHAO, E. C. T., FAHEY, J. J., LITTLER, J. & MILTON, E. J. (1962). *J. Geophys. Res.* **67**, 419-421.

DOWNS, R. T., GIBBS, G. V. & BOISEN, M. B. JR (1990). *Am. Mineral.* **75**, 1253-1262.

DURIF, A., AVERBUCH-POUCHOT, M. T. & GUITEL, J. C. (1976). *Acta Cryst.* B**32**, 2957-2960.

EDGE, R. A. & TAYLOR, H. W. F. (1971). *Acta Cryst.* B**27**, 594-601.

EFFENBERGER, H., KIRFEL, A., WILL, G. & ZOBETZ, E. (1983). *Neues Jahrb. Mineral Monatsh.* **2**, 60-68.

FEI, Y., SAXENA, S. K. & NAVROTSKY, A. (1990). *J. Geophys. Res.* **95**, 6915-6928.

FINGER, L. W., HAZEN, R. M. & PREWITT, C. T. (1991). *Am. Mineral.* **76**, 1-7.

FINGER, L. W., KO, J., HAZEN, R. M., GASPARIK, T., HEMLEY, R. J., PREWITT, C. T. & WEIDNER, D. J. (1989). *Nature (London)*, **341**, 140-142.

FINGER, L. W. & PREWITT, C. T. (1990). *Geophys. Res. Lett.* **16**, 1395-1397.

FLEET, M. E. & BARBIER, J. (1989). *Acta Cryst.* B**45**, 201-205.

FLYNN, J. J. & BOER, F. P. (1969). *J. Am. Chem. Soc.* **91**, 5756-5761.

FUJINO, K., MOMOI, H., SAWAMOTO, H. & KUMAZAWA, M. (1986). *Am. Mineral.* **71**, 781-785.

GASPARIK, T. (1990). *J. Geophys. Res.* **95**, 15751-15769.

GOREAUD, M., CHOISNET, J., DESCHANVRES, A. & RAVEAU, B. (1973). *Mater. Res. Bull.* **8**, 1205-1214.

HAGGERTY, S. E. & SAUTTER, V. (1990). *Science*, **248**, 993-996.

HAZEN, R. M. (1988). *Sci. Am.* June 1988, pp. 74-81.

HAZEN, R. M. (1990). *Physical Properties of High Temperature Superconductors* II, edited by D. M. GINSBERG, pp. 121-198. Singapore: World Scientific.

HAZEN, R. M. & FINGER, L. W. (1982). *Comparative Crystal Chemistry*. New York: Wiley.

HESSE, K. F. (1979). *Acta Cryst.* B**35**, 724-725.

HILL, R. J., NEWTON, M. D. & GIBBS, G. V. (1983). *J. Solid State Chem.* **47**, 185-200.

HORIUCHI, H., HIRANO, M., ITO, E. & MATSUI, Y. (1982). *Am. Mineral.* **67**, 788-793.

HORIUCHI, H., ITO, E. & WEIDNER, D. J. (1987). *Am. Mineral.* **72**, 357-360.

ITO, E. (1977). *Geophys. Res. Lett.* **4**, 72-74.

ITO, E. & MATSUI, Y. (1974). *Phys. Earth Planet. Int.* **9**, 344-352.

ITO, E. & MATSUI, Y. (1977). *High-Pressure Research Applications in Geophysics*, edited by M. MANGHNANI & S. AKIMOTO, pp. 93-208. New York: Academic Press.

ITO, E. & MATSUI, Y. (1978). *Earth Planet Sci. Lett.* **38**, 443-450.

ITO, E. & MATSUI, Y. (1979). *Phys. Chem. Miner.* **4**, 265-273.

ITO, E. & WEIDNER, D. J. (1986). *Geophys. Res. Lett.* **13**, 464-466.

JACKSON, W. E., KNITTLE, E., BROWN, G. E. JR & JEANLOZ, R. (1987). *Geophys. Res. Lett.* **14**, 224-226.

JORGENSEN, J. D. (1987). *Jpn J. Appl. Phys.* **26** (Suppl. 26-3), 2017-2118.

KAWAI, N., TACHIMORI, M. & ITO, E. (1974). *Proc. Jpn Acad.* **50**, 378.

KINOMURA, N., KUME, S. & KOIZUMI, M. (1975). *Mineral. Mag.* **40**, 401-404.

KIRKPATRICK, R. J., HOWELL, D., PHILLIPS, B. L., CONG, X. D., ITO, E. & NAVROTSKY, A. (1991). *Am. Mineral.* **76**, 673-676.

KUDOH, Y., ITO, E. & TAKEDA, H. (1987). *Phys. Chem. Miner.* **14**, 350-354.

KUDOH, Y., PREWITT, C. T., FINGER, L. W., DAROVSKIKH, H. & ITO, E. (1990). *Geophys. Res. Lett.* **17**, 1481-1484.

KUME, S., MATSUMOTO, T. & KOIZUMI, M. (1966). *J. Geophys. Res.* **71**, 4999-5000.

LECLAIRE, A. & RAVEAU, B. (1988). *J. Solid State Chem.* **75**, 397-402.

LIEBAU, F. (1985). *Structural Chemistry of Silicates*. New York: Springer.

LIEBAU, F. & HESSE, K. F. (1971). *Z. Kristallogr.* **133**, 213-224.

LIU, L. G. (1974). *Geophys. Res. Lett.* **1**, 277-280.

LIU, L. G. (1975*a*). *Geophys. Res. Lett.* **2**, 417-419.

LIU, L. G. (1975*b*). *Nature (London)*, **258**, 510-512.

LIU, L. G. (1976*a*). *Nature (London)*, **262**, 770-772.

LIU, L. G. (1976*b*). *Earth Planet. Sci. Lett.* **31**, 200-208.

LIU, L. G. (1976*c*). *Phys. Earth Planet. Int.* **11**, 289-298.

LIU, L. G. (1977*a*). *Geophys. J. R. Astron. Soc.* **48**, 53-62.

LIU, L. G. (1977*b*). *Earth Planet. Sci. Lett.* **35**, 161-168.

LIU, L. G. (1977*c*). *Geophys. Res. Lett.* **4**, 183-186.

LIU, L. G. (1978*a*). *Earth Planet. Sci. Lett.* **37**, 438-444.

LIU, L. G. (1978*b*). *Phys. Chem. Miner.* **3**, 291-299.

LIU, L. G. (1979). *Earth Planet. Sci. Lett.* **42**, 202-208.

LIU, L. G. & RINGWOOD, A. E. (1975). *Earth Planet. Sci. Lett.* **28**, 209-211.

MCHONE, J. F., NIEMAN, R. A. & LEWIS, C. F. (1989). *Science*, **243**, 1182-1184.

MADON, M., CASTEX, J. & PEYRONNEAU, J. (1989). *Nature (London)*, **342**, 422-425.

MAO, H. K., CHEN, L. C., HEMLEY, R. J., JEPHCOAT, A. P. & WU, Y. (1989). *J. Geophys. Res.* **94**, 17889-17894.

MAO, H. K., YAGI, T. & BELL, P. M. (1977). *Carnegie Inst. Washington Yearb.* **76**, 502-504.

MAREZIO, M., REMEIKA, J. P. & JAYARAMAN, A. (1966). *J. Chem. Phys.* **45**, 1821-1824.

MAYER, H. (1974). *Monatsh. Chem.* **105**, 46-54.

MAYER, H. & VOLLENKLE, H. (1972). *Monatsh. Chem.* **103**, 1560-1571.

MEGAW, H. D. (1973). *Crystal Structures: a Working Approach.* Philadelphia: W. B. Saunders.

MODARESI, A., GERARDIN, R., MALAMAN, B. & GLEITZER, C. (1984). *J. Solid State Chem.* **53**, 22-34.

MOORE, P. B. & ARAKI, T. (1974) *Am. Mineral.* **59**, 985-1004.

NADEZHINA, T. N., POBEDIMSKAYA, E. A. & BELOV, N. V. (1974). *Kristallografiya*, **19**, 867-869.

NEVSKY, N. N., ILYUKHIN, V. V. & BELOV, N. V. (1979). *Dokl. Akad. Nauk SSSR*, **246**, 1123-1126.

NEVSKY, N. N., ILYUKHIN, V. V., IVANOVA, L. I. & BELOV, N. V. (1978). *Dokl. Akad. Nauk SSSR*, **242**, 1074-1077.

NEVSKY, N. N., ILYUKHIN, V. V., IVANOVA, L. I. & BELOV, N. V. (1979). *Dokl. Akad. Nauk SSSR*, **245**, 110-113.

NOWOTNY, H. & WITTMANN, A. (1954). *Monatsh. Chem.* **85**, 558-574.

OZAKI, Y., GHEDIRA, M., CHENAVAS, J., JOUBERT, J. C. & MAREZIO, M. (1977). *Acta Cryst.* **33**, 3615-3617.

PARISE, J. B., WANG, Y., YEGANEH-HAERI, A., COX, D. E. & FEI, Y. (1990). *Geophys. Res. Lett.* **17**, 2089-2092.

PAULING, L. (1960). *The Nature of the Chemical Bond.* Ithaca: Cornell Univ. Press.

POST, J. E. & BURNHAM, C. W. (1986). *Am. Mineral.* **71**, 1178-1185.

PREISINGER, A. (1962). *Naturwissenschaften*, **49**, 345.

PREWITT, C. T. & SLEIGHT, A. W. (1969). *Science*, **163**, 386-387.

REID, A. F., LI, C. & RINGWOOD, A. E. (1977). *J. Solid State Chem.* **20**, 219-226.

REID, A. F. & RINGWOOD, A. E. (1969). *J. Solid State Chem.* **1**, 6-9.

REID, A. F. & RINGWOOD, A. E. (1970). *J. Solid State Chem.* **1**, 557-565.

REID, A. F. & RINGWOOD, A. E. (1975). *J. Geophys. Res.* **80**, 3363-3369.

REID, A. F., WADSLEY, A. D. & RINGWOOD, A. E. (1967). *Acta Cryst.* **23**, 736-739.

RINGWOOD, A. E. (1962). *J. Geophys. Res.* **67**, 4005-4010.

RINGWOOD, A. E. (1966). *Advances in Earth Sciences*, edited by P. HURLEY, pp. 357-398. Cambridge: MIT Press.

RINGWOOD, A. E. & MAJOR, A. (1967*a*). *Earth Planet Sci. Lett.* **2**, 106-110.

RINGWOOD, A. E. & MAJOR, A. (1967*b*). *Earth Planet Sci. Lett.* **2**, 130-133.

RINGWOOD, A. E. & MAJOR, A. (1971). *Earth Planet Sci. Lett.* **12**, 411-418.

RINGWOOD, A. E., REID, A. F. & WADSLEY, A. D. (1967). *Acta Cryst.* **23**, 736-739.

RINGWOOD, A. E. & SEABROOK, M. (1962). *Geophys. Res. Lett.* **67**, 1960-1962.

ROBINSON, K., GIBBS, G. V. & RIBBE, P. H. (1971). *Science*, **172**, 567-570.

ROSS, C. R., BERNSTEIN, L. R. & WAYCHUNAS, G. A. (1988). *Am. Mineral.* **73**, 657-661.

ROSS, N. L. & HAZEN, R. M. (1990). *Phys. Chem. Miner.* **17**, 228-237.

ROSS, N. L., SHU, J., HAZEN, R. M. & GASPARIK, T. (1990). *Am. Mineral.* **75**, 739-747.

SAALFELD, H. & KLASKA, K. H. (1985). *Z. Kristallogr.* **172**, 129-133.

SAWAMOTO, H. (1977). *High-Pressure Research Applications in Geophysics*, edited by M. H. MANGHNANI & S. AKIMOTO, pp. 219-244. New York: Academic Press.

SCHELLHAAS, F., HARTL, H. & FRYDRYCH, R. (1972). *Acta Cryst.* **28**, 2834-2838.

SINCLAIR, W. & RINGWOOD, A. E. (1978). *Nature (London)*, **272**, 714-715.

SMITH, J. V. (1982). *Geometrical and Structural Crystallography.* New York: Wiley.

SMITH, J. V. & MASON, B. (1970). *Science*, **168**, 832-833.

SMYTH, J. R. & BISH, D. L. (1988). *Crystal Structures and Cation Sites of the Rock-Forming Minerals.* Winchester, MA: Allen and Unwin.

STEBBINS, J. F. & KANZAKI, M. (1991). *Science*, **251**, 294-298.

STISHOV, S. M. & BELOV, N. V. (1962). *Dokl. Akad. Nauk SSSR*, **143**, 951.

STISHOV, S. M. & POPOVA, S. V. (1961). *Geokhimiya*, **10**, 837-839.

STURA, G. I., BELOKONEVA, E. I., SIMONOV, M. A. & BELOV, N. V. (1978). *Dokl. Akad. Nauk SSSR*, **242**, 1078-1081.

SUBRAMANIAN, M. A., GOPALAKRISHNAN, J. & SLEIGHT, A. W. (1988). *Mater. Res. Bull.* **23**, 837-842.

SUGIYAMA, M., ENDO, E. & KOTO, K. (1987). *Mineral. J.* **13**, 455-466.

SWANSON, D. K. & PREWITT, C. T. (1983). *Am. Mineral.* **68**, 581-585.

THOMPSON, J. B. (1978). *Am. Mineral.* **63**, 239-249.

TILLMANNS, E., GEBERT, W. & BAUR, W. H. (1973). *J. Solid State Chem.* **7**, 69-84.

VICAT, J., FANCHAN, E., STROBEL, P. & QUI, D. T. (1986). *Acta Cryst.* **B42**, 162-167.

VINEK, H., VOELLENKLE, H. & NOWOTNY, H. (1970). *Monatsh. Chem.* **101**, 275-284.

VOELLENKLE, H. & WITTMANN, H. (1971). *Monatsh. Chem.* **102**, 1245-1254.

VOELLENKLE, H., WITTMANN, H. & NOWOTNY, H. (1969). *Monatsh. Chem.* **100**, 79-90.

VON DREELE, R. B., BLESS, P. W., KOSTINER, E. & HUGHES, R. E. (1970). *J. Solid State Chem.* **2**, 612-618.

WADSLEY, A. D. (1964). *Non-Stoichiometric Compounds*, edited by L. MANDELCOIN, p. 111. New York: Academic Press.

YAGI, T., MAO, H. K. & BELL, P. M. (1978). *Phys. Chem. Miner.* **3**, 97-110.

YAGI, T., MAO, H. K. & BELL, P. M. (1982). *Advances in Physical Geochemistry*, edited by S. K. SAXENA, pp. 317-325. Berlin: Springer.

YAMADA, H., MATSUI, Y. & ITO, E. (1983). *Mineral. Mag.* **47**, 177-181.

YAMADA, H., MATSUI, Y. & ITO, E. (1984). *Mineral. J.* **12**, 29-34.